Manipulating nanoscale structure to control functionality in printed organic photovoltaic, transistor and bioelectronic devices

Matthew J Griffith[1,2], Natalie P Holmes[2], Daniel C Elkington[2], Sophie Cottam[2], Joshua Stamenkovic[2], A L David Kilcoyne[3] and Thomas R Andersen[2,4]

[1] School of Mathematical and Physical Sciences, Faculty of Science, University of Newcastle, Callaghan, NSW, 2308, Australia
[2] Centre for Organic Electronics, University of Newcastle, Callaghan, NSW, 2308, Australia
[3] Advanced Light Source, Lawrence Berkeley National Laboratory, Berkeley, CA 94720, United States of America [4] Department of Polymer Science and Engineering, Zhejiang University, Hangzhou Shi, People's Republic of China

E-mail:

matthew.griffith@newcastle.edu.au

Abstract
Printed electronics is simultaneously one of the most intensely studied emerging research areas in science and technology and one of the fastest growing commercial markets in the world today. For the past decade the potential for organic electronic (OE) materials to revolutionize this printed electronics space has been widely promoted. Such conviction in the potential of these carbon-based semiconducting materials arises from their ability to be dissolved in solution, and thus the exciting possibility of simply printing a range of multifunctional devices onto flexible substrates at high speeds for very low cost using standard roll-to-roll printing techniques. However, the transition from promising laboratory innovations to large scale prototypes requires precise control of nanoscale material and device structure across large areas during printing fabrication. Maintaining this nanoscale material control during printing presents a significant new challenge that demands the coupling of OE materials and devices with clever nanoscience fabrication approaches that are adapted to the limited thermodynamic levers available. In this review we present an update on the strategies and capabilities that are required in order to manipulate the nanoscale structure of large area printed organic photovoltaic (OPV), transistor and bioelectronics devices in order to control their device functionality. This discussion covers a range of efforts to manipulate the electroactive ink materials and their nanostructured assembly into devices, and also device processing strategies to tune the nanoscale material properties and assembly routes through printing fabrication. The review finishes by highlighting progress in printed OE devices that provide a feedback loop between laboratory nanoscience innovations and their feasibility in adapting to large scale printing fabrication. The ability to control material properties on the nanoscale whilst simultaneously printing functional devices on the square metre scale is prompting innovative developments in the targeted nanoscience required for OPV, transistor and biofunctional devices.

Keywords: nanotechnology, organic electronics, printed electronics, polymer, biocompatible, semiconductors, large area

1. Introduction

The enormous demand for consumer electronics has gener- ated an urgent need for new hybrid electronic materials that can be readily deposited at low cost over large areas [1, 2]. The global electronics market had an estimated value of more than $1.5 trillion in 2017 [3], with the vast majority of pro- ducts currently fabricated from inorganic semiconductors. Such high demand has created intense interest in printed electronics, a field which focuses on the manufacture of electronic circuits and devices on mechanically flexible sub- strates at high speeds across large areas using cheap roll-to- roll (R2R) processing techniques [4–6]. However, commer- cial realisation of the substantial potential offered by printed electronics requires two critical parallel developments. Firstly, innovative manufacturing techniques that are faster, cheaper and more eco-friendly than conventional methods must be developed [7]. Simultaneously, new electronic materials must be developed that are compatible with these solution-based manufacturing techniques and allow manipulation of the nanoscale architecture of multilayer thin-films to create highly functional electronic devices [8, 9].

Organic electronic (OE) materials have attracted part- icular interest as ideal candidates for printed electronics applications. The suitability of OE materials for this purpose arises from the ability to easily modify their nanoscale che- mical, physical and electronic properties and thereby control their film-forming mechanisms and functionality in electronic devices [10]. Furthermore, it has been recently recognised that organic semiconductors have the unique advantage that the soft carbon-based materials are inherently compatible with the soft, elastic tissue in biological samples. This bio- compatibility enables unprecedented possibilities for bioe- lectronics implants that cannot be accessed with inorganic electronic materials, which the human body often rejects. This emerging field of organic bioelectronics comprises the development and studies of OE devices that operate as translators between the signals and functions of biology and those of electronic processing systems [11]. Due to these advantages, OE materials have been used as the building blocks for nanostructured flexible electronics across a wide- range of novel scientific and commercial applications (figure 1) [13–21].

A common theme across the many research innovations in the OEs space is the requirement for precise material or device nanostructure to be created in order to unlock the desired device functionality or performance [22–24]. This precise control of nanoscale morphology in multilayer OE devices is typically achieved with various carefully calibrated laboratory fabrication and processing techniques [25]. How- ever, controlling the material nanoscale structure and morphology across the large areas during the printing fabri- cation processes required for mass manufacture remains a significant challenge due to the crude thermodynamic levers available in the printing process [26]. The discrepancy between the need for precisely controlled nanostructure in OE devices and the difficulty controlling nanostructure in large- scale printing fabrication is an area that requires the

development of new nanoscience innovations that can be tailored towards the requirements of OE materials and devices prepared using printing fabrication.

In this review we provide an overview of recent devel- opments in the area of printing fabrication of OE materials across size scales varying from fundamental laboratory devices to commercial prototypes. The discussion will be directed towards devices where the optical, electrical or bio- functional properties are deliberately manipulated through nanoscience, including photovoltaics, organic transistors and biofunctional sensing platforms. The focus of the review is to provide insight into various materials and fabrication inno- vations that are targeted towards creating, maintaining and characterising the nanoscale structure of OE materials during large area printing fabrication in order to highlight the improving pathway towards low cost fabrication of flexible OE devices at large scale.

2. Electroactive inks: key materials and properties

A unique aspect of OE research is the ability to solubilise or disperse the OE materials into solvents. These dispersions provide electroactive inks that then enable printing fabrication of functional films. Depending on the desired functionality of the printed device, for instance energy conversion, electrical signal transduction or sensing, the electronic inks can have very different material requirements. One powerful approach to manipulate the electronic functionality of materials is to tune their molecular structure in order to induce inter- molecular forces and other self-assembly mechanisms between molecules that can induce order at the nanoscale. This approach is a widely understood pathway towards manipulating and enhancing a vast range of chemical and physical properties of electronic materials, however, many of these approaches utilise a sophisticated pre-structured tem- plate or precision lithography in order to introduce specific nanostructure into the fundamental materials [27–30]. These approaches are challenging to apply to fabrication via large area printing pathways, where the minimum feature size is limited to the microscale and control of ink thermodynamics is heavily restricted. As such the development of new mate- rials, processing treatments and device fabrication innova- tions are required in order to manipulate the nanostructure of both the materials and devices they are fabricated from. In the following section we outline some of the key materials and structural considerations for OE materials used in printed electronics, highlighting key strategies to modify the mole- cular structure of materials in order to manipulate the elec- troactive ink interactions to create the desired nanostructure and device properties.

2.1. Key material properties for OE devices

The initial interaction with external stimuli such as light, electric fields, chemicals or biomaterials will create charge carrier in the conduction or valence bands of the OE material. The mechanism of free charge carrier generation and transport

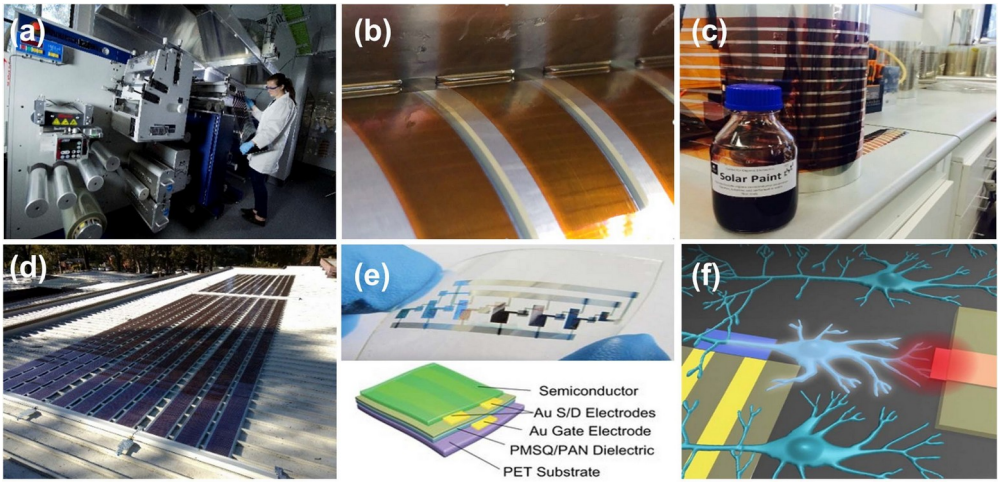

Figure 1. (a) A roll-to-roll coating machine printing OE inks, and (b) image of a dielectric ink being printed onto a semiconducting polymer for OE sensors on a Grafisk Maskinfabrik Solar 1 R2R coater. (c) A functional electronic ink comprised of donor–acceptor nanoparticles for OE devices. (d) Printed flexible light-weight organic solar cells fabricated at the University of Newcastle's Centre for Organic Electronics. (e) A printed transistor device and schematic structure highlighting the precise nanostructuring of the various electroactive layers. Figure reproduced with permission from [12]. Copyright 2012 by Springer Nature. (f) An illustration of electrical stimulation of biological cells in order to interface devices with the human body. Figure reproduced with permission from [11]. Copyright 2012 by Springer Nature.

in organic semiconductors has generated substantial interest, where the lowest energy excited states are strongly bound excitons, which decay before dissociating into free charge carriers with appreciable yield. This problem has been shown to be dependent on photon energy for individual materials [31], which makes choice of the semiconductor critical in order to optimise functionality in a photovoltaic, transistor or biosensing device. Since the movement of charge occurs in localized molecular energy states in organic semiconductors [32, 33], there has been intense research focussing on manipulating the photophysics, photochemistry, and structure/function relationships of organic devices through mod- ifying the nanoscale structure of the electroactive ink materials. Accordingly, it is critical to identify key macroscale ink properties that can be influenced by manipulating nanoscale ink structure.

Substantial research investment has been made over the past decade to enable tunable OE material absorption prop- erties to harvest a controlled portion of incident radiation. The absorption properties in these materials arise predominantly from the energy of the localized highest occupied molecular orbital (HOMO) and lowest unoccupied molecular orbital (LUMO) bands and the molecular ordering between mole- cules, which provides the first design figure of merit for an electroactive OE ink. The energy of the HOMO and LUMO can be modulated by tuning both the length scale of aroma- ticity in molecules and by chemically connecting electron donors and electron acceptors in the same molecule through rational molecular design [34–36]. However, such strategies can lead to strong aggregation of the stacked aromatic groups and sub-optimal material packing. To circumvent this, the aromaticity of the molecules can be manipulated to control electron donor–acceptor interactions whilst simultaneously crafting sterically hindered substituents onto molecules to optimise the molecular packing. This approach has been

employed to achieve both 3-dimensional light harvesting [37, 38] and optimal molecular packing for tuning the crys- tallinity of molecules [25, 39].

Following the creation of free charges, these charges must be swept out of the device. Application of an electric field to organic semiconducting materials containing mobile charge carriers will accelerate the charges, which collide and scatter with defects in the semiconductor lattice to reach an average drift velocity that provides net motion through a material. The drift velocity of the carriers (υ_d) will vary depending on the electric field driving force (E), with a pro- portionality constant between the two given the name of the charge carrier mobility, μ [40]:

$$u_d = mE.$$

The mobility is thus an indication of how fast charge carriers will flow in an OE material, and thus provides a second figure of merit to optimise the electrical performance in OE devices. There are a number of strategies which have shown pathways to improve this charge carrier transport by modulating the molecular packing of the OE materials through improved self- assembly on surfaces creating aligned crystalline grain directions [41, 42], use of additives to direct a more favourable molecular alignment for aromatic overlap of molecular chains [43, 44], or changing the local electrical potential of the molecular environment through the ink sol- vent polarity in order to influence the crystallinity and grain sizes of the electronic materials to achieve faster charge car- rier transport [25, 45, 46].

Finally, the balance between extraction of free charges in the electric field and recombination of electron–hole pairs is critical to OE device performance (figure 2). This kinetic competition can be monitored on the extraction side by measurement of the mobility, whilst the recombination rate can be monitored by measuring the charge carrier lifetime, τ

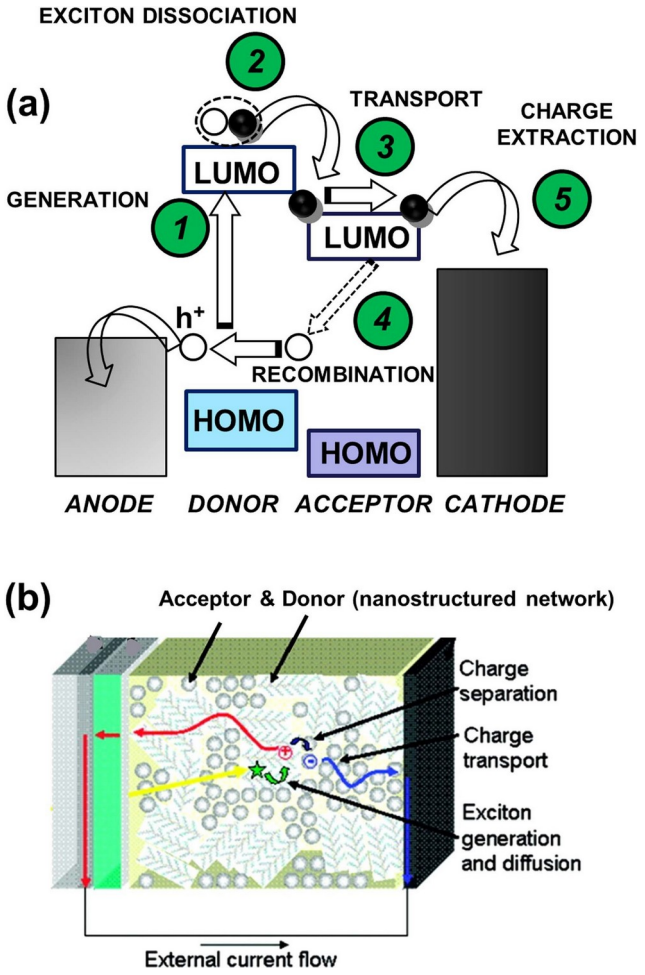

Figure 2. (a) An illustration of the charge generation, exciton dissociation, transport, recombination and extraction processes critical to OE devices. (b) A schematic illustration of a nanos- tructured network employed to promote transport and restrict recombination. Figure adapted with permission from [47]. Copyright 2010 by American Chemical Society.

[48], which provides a third figure of merit for characterizing dynamic charge carrier processes in OE devices. The recombination can be tuned through clever design of the ink components, introducing chemical dopants that electrically screen charges from each other at the nanoscale [49]. The competing charge transfer processes can also be optimised by creating nanostructured two or three phase donor–acceptor blends where the nanostructure is engineered through control of the material blending parameters to ensure distribution of charge transport across different material phases and thus limit recombination [9, 50–52]. Another successful approach is to separate the signal carrier duties between ions and electrons in mixed bioelectronics systems through the intro- duction of ionic carriers such as nerve cells or polyionic materials [10, 11, 53, 54].

2.2.Semiconducting polymers

Polymer and small molecule organic semiconductors differ from their inorganic counterparts in their synthetic versatility.

Consequently, the conduction of electrical charge in organic polymers has attracted great attention by scientists and engi- neers in recent years. Of particular note is that the polymer inks can conduct signals in the form of electronic charge in their molecular bands, but also in the form of ions, which may migrate through an organic solid material if enough cross section (i.e. pore size) and molecular dynamics (e.g. flex- ibility) are provided by the conducting solid [10, 11]. Polymer molecules can also be readily functionalised by various nanoengineering pathways in order to impart tunability to their optical, electronic, mechanical and physical properties through induced intermolecular interactions [55]. Of these polymer inks, three standard workhorse materials are heavily utilised in OEs. Polypyrrole (PPy) has been employed in solar cells, where the crystallinity of the ink was tuned by utilizing a block copolymer and solvent annealing approach to improve the packing of the polymer backbone in cast films and thus improve the mobility of the material [45]. Deliberate nanostructure has also been introduced to PPy inks through printing the material onto nanostructured 3D printed mole- cular scaffolds to enhance the carrier mobility [56, 57]. An alternative strategy that has been reported is to utilise the printing fabrication route to deposit patterned arrays where the surface roughness can be modulated by manipulating the size, shapes and solvent treatments of the arrays. This had led to advances in sensitivity of PPy devices [58] and led to an exciting approach for controlling the electro-stimulation and growth of cells in bioelectronics probes through the nanos- tructured pattern of the PPy ink layers [59], which controlled the degree of cell adhesion through the nanoengineered sur- face roughness of the ink and promoted the controlled growth through the patterning of the polymer ink.

Polyaniline (PAni) is another material that has been heavily used in organic sensors and transistors. This academic interest in polyaniline arises from its unique number of redox states and doping mechanisms when compared to other con- ducting materials. PAni initially had limited use due to poor reaction control and processability associated with conven- tional morphologies, however a pioneering synthetic approach to control the chemical reaction at the interface between two immiscible liquids have allowed the fabrication of nanofiber inks [60]. These PAni nanofibers subsequently demonstrated increased processability, higher surface area, and improved consistency and stability in aqueous disper- sions. Furthermore, the conductivity and wettability of these PAni inks can be tuned by modulating the surface roughness through utilising dopant additives in the synthesis with varying acidic strength [61]. These tuned nanostructured properties led to the use of these inks to enhance electron transfer kinetics in solar cells [62], and more recently as a biocompatible substrate that has been safely inserted into animals and shown to stimulate nerve and cell growth [63, 64].

Poly(3-hexylthiophene) (P3HT) is perhaps the most widely used semiconducting polymer donor material due to heavy usage in the large field of organic photovoltaic (OPV) devices, with advantages ranging from easy synthesis to high charge carrier mobility, good processability and stability to

photo-degradation (figures 1(b) and (d)) [65]. The compara- tively straightforward synthesis and availability of monomer has for some time positioned P3HT among a limited group of donor polymers that are suitable for the large-scale com- mercialisation of OPVs [66]. The hole mobility of P3HT has been shown to be tunable across the range of 10^{-4}–10^{-1} cm^2 V^{-1} s^{-1} by controlling the molecular weight [66, 67], regioregularity [68] and interchain polarity through organic acid dopants [69], leading to applications in transistors and sensors [70] where the output sensitivity is dependent on these doping mechanisms. Electroactive P3HT inks have also been shown to have their electronic and ionic conductivity modulated by the local humidity and polyionic additives [71]. This has led to recent deployment of these inks in bioelec- tronics devices that have photostimulated cells and dis- tinguished the signals through these differing ion and electron conduction pathways [72].

Outside of these three materials, substantial research investment has been made over the past decade to develop a range of semiconducting polymers which allows tunable absorption properties to modulate the HOMO-LUMO gap [73]. Modulation of this property is of great interest in photovoltaics, as it allows a greater harvesting of the solar spectrum and leads to higher device photovoltages, which arise directly from this HOMO-LUMO gap. Tuning these polymer properties whilst maintaining optimum thermodynamic energy transfer pathways between donor and acceptor material components presents one of the most heavily studied avenues of OE materials research [38, 74, 75]. Several synthetic strategies have been developed and proven to be very effective, including: (a) nanoscale self- assembly of the polymer backbone using alternating electron-deficient (acceptor) and electron-rich (donor) units to form donor–acceptor copolymers; (b) stabilising the quinoid reso- nance structure; (c) incorporating strong electron withdrawing substitutes such as fluorine atoms or carbonyl groups, and (d) attaching conjugated side chains on the polymer main chains [76]. These approaches have led to a range of new low band gap polymer materials, including poly[2,6-(4,4-bis(2-ethyl- hexyl)-4H-cyclopenta[2,1-b;3,4-b′]dithiophene)-alt-4,7-(2,1,3- benzothiadiazole)] (PCPDTBT), poly[(4,4′-bis(2-ethylhexyl) dithieno[3,2-b:2′,3′- d]silole)-2,6-diyl-alt-(2,1,3-benzothiadia- zole)-4,7-diyl] (PSBTBT), poly[[4,8-bis[(2-ethylhexyl)oxy] benzo[1,2-b:4,5-b′]dithiophene-2,6-diyl] [3-fluoro-2-[(2-ethyl- hexyl)carbonyl]thieno[3,4-b]thiophene-diyl]] (PTB7) and poly [(thiophene)-alt-(6,7-difluoro-2-(2-hexyldecyloxy)quinoxaline) (PTQ10) that have seen the record power conversion efficiency in OPV devices climb from 4% in the early part of the century to over 15% today through modulating the charge generation and mobility by systematically altering the HOMO-LUMO gap [77–81]. However, the additional synthetic complexity of some of the materials required to produce such device performances places an economic limit on the scale at which they can cur- rently be produced that is well below the kilogram scale required for commercialisation of these materials [66, 82]. Consequently one of the major challenges with new semi- conducting polymers is to maintain the optimum optoelectronic properties for high device performance whilst balancing simple synthetic design. The low cost of PTQ10 synthesis and the

thickness insensitivity of PTQ10-based OPV devices positions this polymer as an outstanding candidate for printing of OPV for commercial applications.

2.3.Small molecule electron acceptors

Fullerenes are a class of organic semiconductors well-suited to act as electron acceptors due to a high electron affinity and exceptional charge mobility, making them desirable for thin- film OE applications such as field-effect transistors and organic solar cells. Despite their attractive material properties, a significant drawback of the pure C_{60} and C_{70} materials is the poor processability in organic solvents, which places restric- tions on the quality of electroactive ink formulations prepared from these solvents [74, 83]. This issue can be addressed by a targeted nanoassembly approach where solubilizing moieties are appended to the fullerene cage, which has led to the class of materials most often employed in printed electronics [84]. However, these approaches create a fullerene ink with sub- stantially reduced electron mobility and a strong thermo- dynamic drive towards crystallization into large phase separated domains. Recently, fullerene inks with material properties that lead to more favourable device nanostructure have been enabled by targeting a thermodynamically favourable mixture of pure fullerenes or crude (unpurified) isomers. Blending of pure fullerene cages of different sizes without solubilizing substituents was shown to control the entropy of dissolution and provide inks with control of the domain sizes that increase material mobility and lead to a more desired amorphous nanostructure without phase separation [85]. Furthermore, blending of the solubilized forms of fullerene in a highly controlled and directed fashion was also shown to produce a high-performance ink that can be prepared at low cost on a large scale as it negates the need for expensive purification [86], opening up avenues for large scale, low cost printing.

Whilst fullerene inks have dominated the field of printed electronics, there has also been rapid development in the emerging class of non-fullerene acceptors (NFAs) that have attracted interest due to the advantages of low cost synthesis, broad and strong absorption, and high morphological stability [87]. NFA materials include both small molecules, for example ITIC, ITIC-Th, IOTIC-2F, IDIC, IFIC-o-4F, o-IDTBR, IEIC, IDTBR, IDFBR [65, 87–89], and polymers, for example N2200 and PNDI-T10 [90]. These small mole- cules offer exciting approaches based on traditional supra- molecular chemistry and self-assembly to modify the molecular properties of the ink in order to improve device functionality. Modulating the structure of perylene diimide dimers with substituents through manipulation of the alky- thienyl position was shown to systematically control the aggregation of the small molecule in blended films, leading to enhanced solar cell performance with reduced parasitic charge losses [91]. Furthermore, introduction of a co-oligomer into the same perylene acceptors was shown to induce a highly ordered slef-assembled donor–acceptor lamellae structure which greatly enhanced charge mobility in devices [92]. Recently this approach has been extended to controlling

molecular orientation to induce 2D nanostructure through the ink formulation, synthesizing molecules that utilize designed intermolecular interactions such as hydrogen bonding and charge-transfer complexes to control molecular orientation and ordering in 2 dimensions [81, 93] within the thin printed films of fabricated devcies.

2.4. Printable electrode materials

Printable electrode material inks are growing in popularity, and indeed are a required component of flexible electronic devices as highly conducting electrodes. Amongst these materials, there are very few successful elements that have arisen as the basis of conducting electrodes that can be deposited at low processing temperatures. Silver (Ag) is by far the most dominant [94]. Printable Ag electrodes are gaining use as air-stable high-work-function metal that can be easily formed using printing and coating technologies to simplify and lower the manufacturing cost of electronic devices [95]. Such inks are synthesized from ionic metal precursors or salt compounds dissolved in a solvent that are subsequently reduced to metallic silver nanocrystal building blocks during printing fabrication [96]. The silver nano- particulate ink can be modified through chemical synthesis or thermodynamic processing to adopt a range of shapes, from spherical particles to triangular or square particles and, more recently, elongated nanowires [97–99]. Manipulation of the particle shape leads to inks in which the print parameters such as viscosity, surface tension and boiling point are able to be finely tuned [100], leading to modulation of the electrical resistivity [101, 102] and the optical transparency [103] to optimise device functionality as transparent conductive electrodes. However, a major drawback of silver electrodes for biofunctional printing and devices is that the material itself is cytotoxic and will destroy a wide range of active biological components [104]. Thus other emerging inks and materials must be utilised for biocompatible devices.

Carbon nanomaterials, including single and multiwalled nanotubes, graphene and carbon black nanoparticles have attracted substantial interest in recent years [105–107]. These carbon materials have the advantage of being extremely low cost and light weight, and readily amenable to physical or chemical treatments that can be used to tailor a range of functional properties [108]. However, the carbon materials often require high temperature processing and can contain impurities and defects that reduce electrical conductivity and may be toxic to biological components [109]. The discovery of solution processable graphene and carbon black nano- particles has led to a variety of printable inks where these properties can be tuned for device functionality [110]. Recent advances in this area include the fabrication of 3D nanostructured electrodes with high surface area and electro- chemical activity where this structure was induced by freeze drying a self-assembled reduced graphene oxide ink [111]. Further advances include the addition of specific polymer and small molecule co-absorbers in specific ratios that interact with the carbon inks to direct intermolecular forces and create free-standing electrodes with either a high mechanical

integrity or high electrical conductivity and surface area depending on the additive ratio [112–114]. Excitingly, control of the nanostructure through such techniques has shown recent progress in stimulating biological samples to grow in a controlled fashion, proving both the efficacy of carbon elec- trodes for biofunctional printing and its amenity to tuning device functionality through controlling the ink nanoscale structure and properties [11, 109, 115],

2.5. Printable biofunctional components

Bioelectronics, the convergence of OE materials and devices with biology, is one of the fastest growing areas in materials science. This interest arises from the unique ability of carbon- based semiconducting inks to simultaneously provide the distinctive combination of mechanical and electrical proper- ties required by many biomaterials. Firstly, OE materials present soft and flexible surfaces that are inherently compa- tible with soft flexible carbon-based biomolecules [116]. Additionally, their semiconducting electrical properties also allow the reversible transmission of biological signals or the stimulation of biological tissues [117]. However, much like the OE materials and devices with which they are integrated, many biomolecules must adopt a sophisticated 3D nanos- tructure in order to deliver their desired functionality. Main- taining such nanostructure during large-scale printing fabrication is a substantial challenge that has only recently begun to be addressed. Bioprinting aims to produce nanoen- gineered biofunctional inks in a mechanized, organized, and optimized manner. Various biomaterials and techniques have been utilized to print biological constructs in different shapes, sizes and resolutions (figure 3) [118]. One of the most com- mon pathways is the deposition of complex scaffolds such as hydrogels and polymers using sophisticated 3D printing that are then coated with biofunctional inks into compatible OE material matrices. This approach allows the complex graded designs that are a hallmark of biological materials to be reproduced on nanoengineered supporting OE scaffolds [119, 120] through either self-assembly or direct ink writing techniques [121, 122]. For large scale printing, biofunctional devices have also been prepared by integrating sensing components and cells with OE materials through inkjet and flexographic printing. These approaches have successfully demonstrated an ability to pattern enzymes and proteins for biosensing and drug delivery with microscale resolution [123, 124]. Organic bioelectronics can also be used to reg- ulate the physiology and processes of cells, tissues, and organs in a chemically specific manner and at high spatio- temporal resolution [11]. Several reports of cell growth and stimulation on OE semiconductors have begun to emerge, where the precise nanostructure of the OE materials allows the controlled growth in preferred directions [59, 125], or specific manipulation of cell growth in 3D space through optical and electrical signals where the spatial resolution is created by controlling the underlying nanostructure of the OE stimulation platform [72, 126].

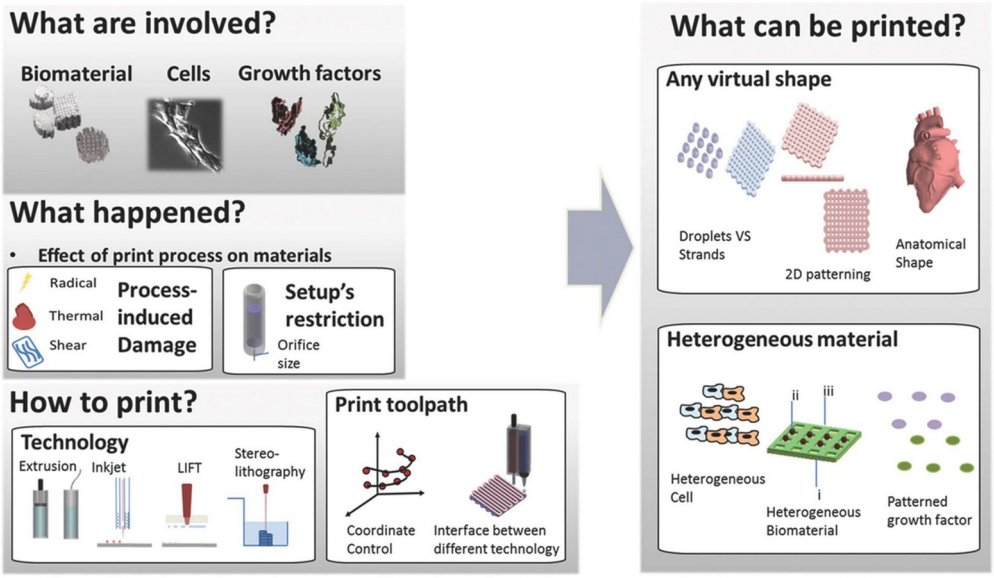

Figure 3. A schematic overview of various materials, manufacturing and nanoscale patterning considerations encountered in the printing of biofunctional materials. Figure reproduced with permission from [118]. Copyright 2016 by John Wiley and Sons.

3. Controlling and measuring printed OE material morphology

The nanostructure of material components in OE devices, often referred to as the material morphology, is fundamentally complex. Heterogeneities often exist across multiple length scales, from millimetre to micrometre to the sub-nanometre scale [55]. Organic semiconductors differ from inorganic semiconductors in that charge carriers formed upon absorp- tion of light or transfer of excited state energy are tightly bound as excitons by electrostatic forces [127]. These excitons can only diffuse a very short distance (~10 nm) prior to relaxation, and must be split in photovoltaic and photo-induced biosensing devices. This process is typically achieved by intermixing donor and acceptor semiconducting inks on the nanoscale such that all created charges are always within 10 nm of an interface [128]. Furthermore, once created in a photovoltaic, transistor or biosensing device, the free charges typically have reduced mobility through the OE materials, where the transport occurs through hopping between strongly localized states [129]. This problem is addressed by modulating the semiconductor crystallinity through its nanoscale morphology in order to maximize the mobility. Whilst these processes have been well-established at the laboratory scale through complex solvent and thermal treatments, they cannot be transferred to printing fabrication techniques, where the structure-function relationships between morphology of electrically active layers and device performance must be re-established to account for the lim- itations of printing equipment and processing control. Here we provide an overview of the key factors affecting morph- ology of common materials employed for OE devices and the strategies that can be utilized to modulate these factors by tuning OE material nanostructure during printing fabrication.

3.1. Tuning morphology using fabrication thermodynamics

Control of OE material morphology at the nanoscale has most often been achieved in carefully controlled laboratory envir- onments through tuning the thermodynamic processing levers involved in the fabrication process. The major factors influ- encing BHJ film morphology have been shown to include material miscibility (often the donor and acceptor material are immiscible to some degree) [130–132], the deposition solvent composition (boiling point, vapour pressure, relative solubi- lity of the donor and acceptor [52], and additives [43]), the thermal annealing conditions [133], and the semiconducting material crystallinity [79].

The choice of solvent and the use of high boiling point (and low vapour pressure) additives in the film coating pro- cess is one area where substantial progress has been made in influencing the nanoscale morphology of materials in printing fabrication. Organic semiconductors may preferentially segregate to the air/film interface or the film/substrate interface depending on the surface energy of the organic semiconductors in comparison with that of the underlying sub- strate [55]. This segregation influences the lateral (and also vertical) film morphology and consequently the performance of the photovoltaic devices [52]. When printing organic semiconductors from solution, rapid solvent evaporation can either inhibit or induce molecular ordering, selectively lock- ing molecules into kinetically-trapped states. Varying the solvent identity induces a well known Maringoni (coffee- ring) drying procedure where solids are distributed non-uniformly across a 2D printed layer due to a gradient of the surface tension. Varying the solvent ratio in organic solvent mixtures has been utilized to deliberately control the degree of Maringoni drying, thus controlling the thickness of OE semiconducting films between 70 and 250 nm in materials that could otherwise not be printed below a thickness of 150 nm. This procedure also produces subsequent alterations

in the film surface roughness between 2 and 10 nm [134, 135]. These changes in surface roughness and thickness have produced tunable wettability that controls the intermix- ing at multiple neighbouring layers in photovoltaic and transistor devices to improve the degree of charge transport through the differing layers [136]. Solvent additives can also been used as post-processing treatments to control material crystallinity and nanoscale domain size. Selective coating of films with organic solvents that are semi-permeable in the underlying material was shown to modulate the crystallinity and phase separation in printed solar cells, leading to high performance for an optimal mixture that balanced crystallinity formation whilst maintaining domains at a size scale of the order of 10–20 nm [137, 138]. In organic transistors, judi- cious choice of deposition and washing solvents were shown to induce high crystallinity and large domain sizes that improve the charge carrier mobility by orders of magnitude [139]. Solvent washing of biocompatible printed PEDOT:PSS films with ethylene glycol has also been shown to induce a high degree of crystallinity [140]. This discovery was utilized in an elegant study demonstrating the controlled crystallinity increases through modulating the amount of co-solvent could enhance electrical conductivity but impede ionic conductivity in a highly tunable fashion, thus tuning the material for optimum biosensing which uses ionic signals for biointerfa- cing and electrical signals for detection [141].

Molecular ordering is central to charge carrier mobility in OE materials, and another major target of tuning the morphology during printing fabrication. Charge carriers are transported through π-orbital overlap of conjugated molecules in organic semiconductor films, and hence the ordering and alignment (crystallisation) of conjugated molecules over sig- nificant distances in the active layers is instrumental in facilitating π-orbital overlap and allowing efficient charge transport from molecule to molecule [55]. In many OE devices such crystallinity is typically controlled through a precise thermal annealing treatment, however, the temper- ature precision across large areas in convection ovens employed in high throughput printing techniques is poor and leads to a loss of crystallinity control [142, 143]. One approach to circumvent this is to apply direct heating control to the printing equipment, such as metal drums and rollers. Heating the backing roller onto which OE inks are deposited in a controlled fashion has been shown to substantially improve both photovoltaic [144] and transistor device per- formance [145]. This improvement is achieved by fine-tuning the rate at which inks dry and controlling the kinetics of the glass transition in the molecules to induce nanoscale control of the semiconducting material crystallinity and domain size. Such treatments have been shown to control the functionality by providing substantially enhanced charge mobility in the fabricated devices [146]. This process can also be fast-tracked in high-speed printing fabrication with an infrared flashlamp to provide precision control by instantly freezing in a desired nanoscale morphology through micrsoecond pulses [147]. Recently a sophisticated system has been demonstrated that independently controls both the printing head temperature and the substrate roller temperature when printing multiple

solution layers sequentially. This approach provides exquisite thermal control, providing a highly ordered crystalline semi- conductor that produced printed photovoltaic devices of a record 12% efficiency [4].

3.2. Nanostructuring the electroactive inks

OPV, transistor and biosensing devices require precisely ordered multilayer films to induce functionality. For photo- voltaics and optical biosensors these films require a bicon- tinuous donor–acceptor interpenetrating network for the transport of holes and electrons to their respective electrodes [148], whilst in transistors and electrochemical biosensors these require semiconductors and structured dielectrics to control ion flow and electric field-induced conductivity [149]. In both cases, the ink materials require characteristic nan- ometer length scales of phase-separated domains. One way to achieve this is through the blending of multiple component materials into the desired electroactive ink prior to deposition. In photovoltaic devices this creates a three-phase photoactive layer morphology, where the size scale can be modulated through judicious selection of additive components. Such an approach can control molecular alloying [150] and inter- molecular forces [151] in order to create nanoscale intermixed domains maximizing interfacial surface area for exciton dis- sociation, nanoscale pure donor domains for hole transport, and nanoscale pure acceptor domains for electron transport [130, 152]. In transistor devices the additive component can be introduced directly into either the dielectric or semi- conductor material in order to create a sensing device. The additives disrupt the dielectric or semiconductor material structure, introducing ions, dopant or electronic carriers in a controlled fashion as the device performance is particularly sensitive to the physical properties of the two interfaces, including channel/electrolyte and gate/electrolyte interfaces [153]. This approach is particularly appealing for biofunc- tional sensors since introduction of biomaterials in the ink can lead to separation of molecules across tens of nanometers at the critical interfaces and introduce the critical dark and bias current difference required for successful sensing [154, 155]. Another approach receiving strong interest for tuning device functionality through controlling the nanostructure of organic electroactive inks is to pre-engineer multi-component nanoparticles as the fundamental ink. Controlling OE material nanoscale structure and morphology across large areas during printing fabrication remains a significant challenge due to the limited thermodynamic levers discussed previously [156]. One potential avenue to circumvent this challenge is to create discrete nanoparticles where the multi-phase structure is imprinted through chemically directed assembly using sur- factants prior to casting the active films [157, 158]. Not only does this approach allow dispersal of the OE nanoparticles into greener solvents such as water and alcohols through the surface-adsorbed surfactant molecules, it also ensures that the thermodynamic control of film morphology is decoupled from the printing process. This nanoengineering approach enables the dual benefits of exquisite nanoscale film structure and low cost, large area printing of electronic devices to be

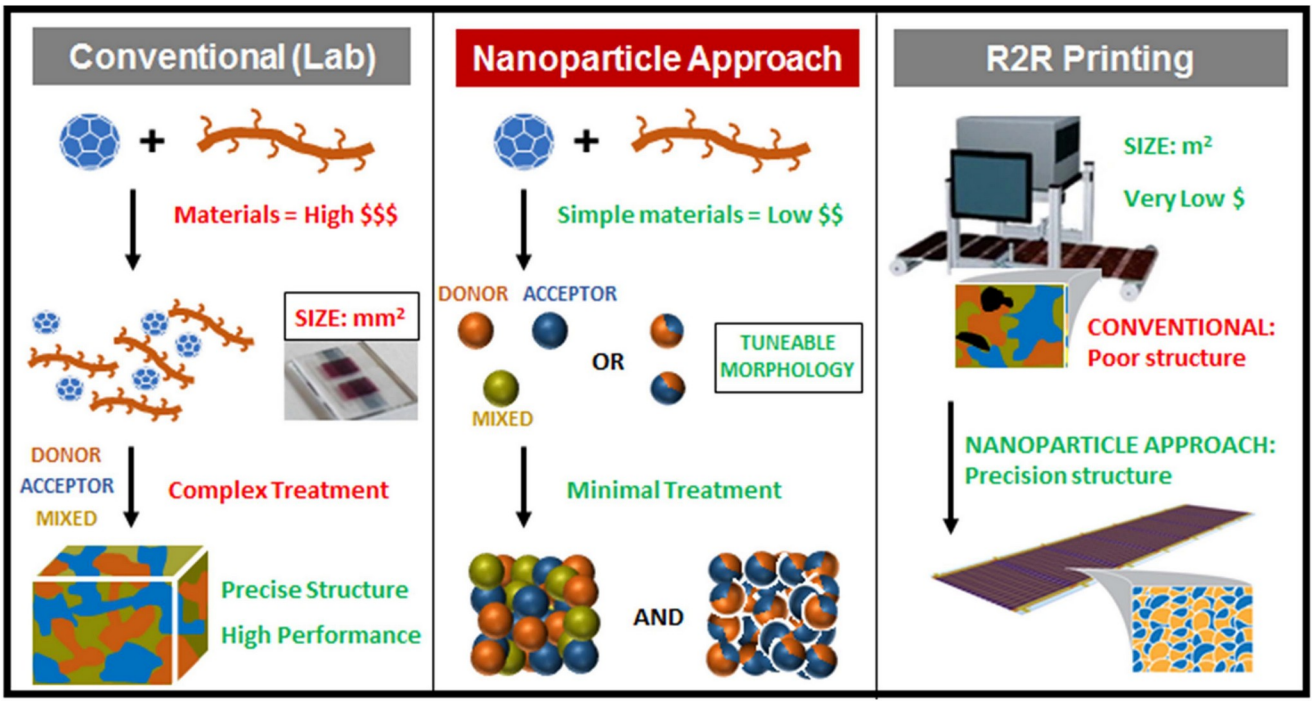

Figure 4. An illustration showing the benefits of nanoparticulate inks that remove the need for complex thermodynamic treatments required to achieve precise nanoscale structure in conventional OE materials that do not scale to R2R printing.

simultaneously realized (figure 4) [157, 159, 160]. Polymer (or macromolecule based) nanoparticle preparation methods fall under two main categories, (1) post-polymerisation dis- persion of pre-synthesised polymers (or secondary dispersion)
[161] and (2) polymerisation in disperse heterophase systems. Post-polymerisation dispersion of pre-synthesised materials comprises two major routes utilised by the OE research community, namely (i) the miniemulsion nanoengineering approach enables the dual benefits of exquisite nanoscale film structure and low cost, large area printing of electronic devices to be simultaneously realized (figure 4) [157, 159, 160]. Polymer (or macromolecule based) nano- particle preparation methods fall under two main categories,
(1) post-polymerisation dispersion of pre-synthesised poly- mers (or secondary dispersion) [161] and (2) polymerisation in disperse heterophase systems. Post-polymerisation disper- sion of pre-synthesised materials comprises two major routes utilised by the OE research community, namely (i) the miniemulsion method and (ii) the nanoprecipitation method. Nanoparticles of binary blends of organic semiconducting polymer donors and fullerene and small molecule acceptors synthesised via the miniemulsion method encompass various morphologies depending on the specific blend ratio between the semiconducting materials, and also the degree of surfac- tant employed. Variation of these parameters can system- atically create either a core–shell [162–167], a pristine [157, 168, 169], or a molecularly intermixed [170, 171] nanoparticle, and can also alter the shape of the particles [172]. This nanoparticulate ink approach offers a unique pathway towards creation of the optimum three phase mat- erial blends composed of pure and intermixed phases, as the charge separation is strongest in the intermolecularly mixed

nanoparticles, whereas the charge mobility is much higher in the core–shell and pristine nanoparticles where crystallinity is much higher. Blending each of these nanoparticles into the electroactive ink then creates an optimum gradient of material mixtures to tune the charge separation and mobility.

Nanoparticles of binary blends of organic polymer P3HT and acceptor ICBA or $PC_{61}BM$ semiconductors synthesised via the nanoprecipitation method are reported to possess only an intermixed morphology [160, 173, 174]. Such an approach deposits organic solutions of semiconductors into an ortho- gonal solvent, where the rate of addition and temperature of the non-solvent control the size of the semiconducting parti- cles as they precipitate from solution into the orthogonal solvent. Careful tuning of these features can provide blended nanoparticles of the optimum length scale for OE devices. In a breakthrough towards large area printing production, both the uniformity and reproducibility of these nanoparticulate inks were subsequently improved by using high-throughput robot-based synthesis [160].

The major advantages of this nanoparticle approach to controlling the structure of semiconducting materials is that there is a high degree of control over both material size and composition in order to pre-set the material domain size and electrical properties in the printed OE thin films. For example, the particle size can be customised to match the exciton dif- fusion length in organic semiconductors, in order for the feature size in the printed OE film to match the exciton dif- fusion length. Marks *et al* demonstrated this by synthesising P3HT:$PC_{61}BM$ nanoparticles of diameter 32 nm using the miniemulsion method, achieved by varying the surfactant concentration during synthesis [170]. Varying nanoparticle size can also be achieved by decreasing the concentration of

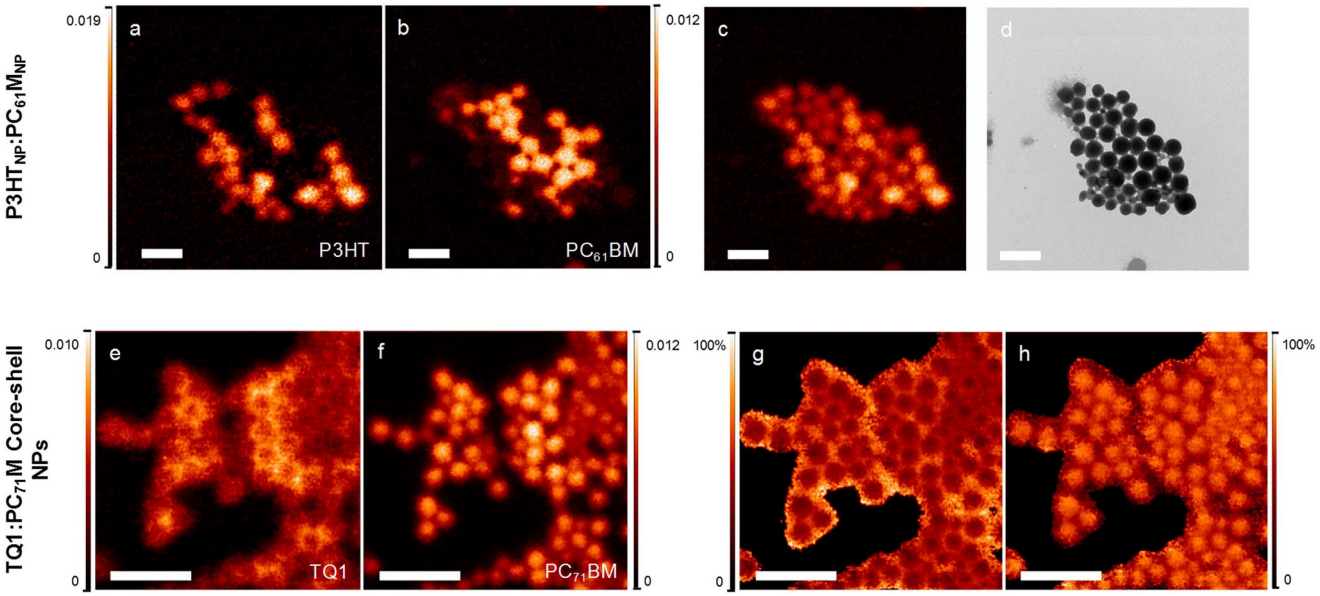

Figure 5. STXM mass plots showing concentration of (a) P3HT, (b) $PC_{61}BM$, and (c) P3HT:$PC_{61}BM$ combined of pristine $P3HT_{NP}$ and pristine $PC_{61}BM_{NP}$ collected at beamline 5.3.2.2 of the Advanced Light Source. (d) Position-matched TEM for the $P3HT_{NP}$:$PC_{61}BM_{NP}$ cluster. STXM mass plots of (e) TQ1, (f) $PC_{71}BM$ for 1:3 TQ1:$PC_{71}BM$ core–shell nanoparticles, and corresponding STXM fractional composition maps showing the concentration of (g) TQ1 and (h) $PC_{71}BM$. Scale bars are 600 nm. For mass plots (a)–(c), (e)–(f) the colour scale bars indicate concentration of component in mg cm^{-2}.

semiconducting material in the miniemulsion oil phase, as Xie *et al* [175] reported for the PDPP5T-2:$PC_{71}BM$ nanoparticle system. Furthermore, there is merit in synthesising separate nanoparticles of donor and acceptor, that is pristine nano- particles, prior to their co-assembly into a film, in order to engineer a photoactive layer with targeted pure bicontinuous percolation pathways of pre-set size. These structures also enable the formation of domains with well-defined contacts (interfaces) between the electron and hole conducting domains [168]. Controlled thermal annealing can then be applied to generate a third intermixed phase, converting a two-phase microstructured film into a three-phase micro-structured film, with phases designed for exciton dissociation (molecularly mixed phase), as well as phases designed for hole transport (pure donor phase) and electron transport (pure acceptor phase) [162].

A temperature-mediated critical micelle concentration (CMC) switching strategy of nanoparticle synthesis emerged in 2018 and authors reported a new record conversion effi-ciency of 7.5% for organic nanoparticle photovoltaic devices [174]. The necessity for surfactants in stabilising nanoparticle dispersions was for some time limiting the maximum achievable device performance due to their parasitic insulat- ing properties in the film, however, the CMC switching strategy employed by Xie *et al* has enabled the stripping of excess surfactant from aqueous colloidal dispersions. This synthesis method is an adapted nanoprecipitation technique, where the micelle forming poloxamer, Pluronic F127, was selected to stabilise the nanoparticles directly after precipita- tion. Importantly, the excess surfactant is controlled by temperature modulation, where lowering the temperature drops the colloidal dispersion below the CMC so that free and loosely bound poloxamers can be removed, this leaves behind

almost surfactant-free nanoparticles for fabrication of OE devices.

The nanoscale distribution of materials in these nano- particles and structured films can be probed using sophisti- cated x-ray techniques. The synchrotron-based soft x-ray technique of scanning transmission x-ray microscopy (STXM) offers spatially resolved chemical contrast at the nanoscale, by utilising the chemical sensitivity of near edge x-ray absorption spectroscopy [176]. STXM employs a monochromatic x-ray beam, which provides chemical map- ping on the nanometre scale throughout the bulk of organic thin films and map out the degree of intermixing of such materials in photovoltaic, transistor and biofunctional sensing devices. For the nanoparticle inks discussed in the previous section, STXM is one of the only techniques available to directly probe the intra-particle nanostructure, which can be achieved on a sub 30 nm length scale [177]. STXM was indispensable in the investigation of thin film morphology when engineering two-phase and three-phase microstructures from water-based colloidal dispersions of $P3HT_{NP}$ and $PC_{61}BM_{NP}$ (figures 5(a)–(d)) [162]. In addition, STXM enabled the composition of domains to be calculated for core– shell nanoparticles of TQ1:$PC_{71}BM$ (figures 5(e)–(h)), showing the nanoparticle shells to be TQ1-rich (70%–85% TQ1) and the nanoparticle cores to be $PC_{71}BM$-rich (75%– 90% $PC_{71}BM$) [164], and allowing a quantitative modelling of charge transport that enabled a pathway back to rational design to optimise the nanoparticulate printing synthesis in order to maximise electronic device performance. Such x-ray probes are also one of the only tools that can be successfully upscaled onto roll-to-roll printing equipment, providing the first real-time feedback on optimum morphology during printing fabrication of OE devices. Such equipment has been

used to determine the optimum drying and thermal treatment conditions for obtaining nanoscale crystallinity with con- trolled domains in polymer photovoltaic and transistor devi- ces [178], determining the influence of solvent drying kinetics on film nanostructure and performance [144, 179], and ver- ifying self-assembly of precursor materials into aligned lamellae structures optimized for mobility in solution pro- cessed photovoltaics [180].

4. Applications of printed OE devices with tuneable nanostructure

4.1. Different scales of printing fabrication

In order to address the stark gap between numerous innova- tive laboratory scale achievements and the limited industrial scale production of OE devices, a consideration of the upscaling of the printing fabrication pathway is required. The major limitation in translating the sophisticated electroactive ink nanostructures and high device performance demonstrated on the laboratory scale for a variety of OE materials through to their full potential as flexible large area products is the radically different fabrication tools and environment required to work on this industrial scale [181]. Consequently, the structure-function relationships that have been so carefully elucidated on the laboratory scale over decades for many of the photovoltaic, transistor and biosensor devices do not translate directly to the larger scale, explaining the significant gap between the high performance of small scale devices and the lack of larger scale examples [182]. The translation of OE technology to printing procedures compatible with mass manufacture are often analysed independently using fabrica- tion tools optimized for various printing scales [144]. In general, these can be split into 3 distinct arenas depending on the size scale of the devices produced and the corresponding difficulty of fabricating functional devices with a controlled nanostructure approaching that achievable in the highly controlled laboratory environment (figure 6). The first approach is to develop a transition from laboratory equipment such as spin coaters and precision vacuum deposition systems to new printing equipment at the small scale (device areas below 1 cm^2). This approach is often characterised by printing tools such as inkjet printers, and aims to rapidly examine the ability of printing procedures and ink formulations to trans- ition sophisticated material nanostructures from vacuum deposition in the laboratory to printing fabrication with a more limited thermodynamic control [6, 135, 183, 184]. This approach is typically the most popular as the equipment is relatively low cost and the innovations can be rapidly developed to screen for compatibility with printing fabrica- tion. The second approach is to investigate an intermediate scale where the device area is larger than 1 cm^2 but below 1 m^2. Research in this space will often employ tools like screen printing, and can attempt to fabricate some of the device components using a R2R process to directly demon- strate mass manufacturing capabilities [185–187]. These studies typically combine R2R processes with standard

laboratory fabrication, although the findings are more readily applicable to full R2R fabrication than the first approach as they begin to address issues that are specific to large area fabrication equipment. The third approach is to fabricate large devices (areas above 1 m^2) using only fully R2R processes [103, 156, 188, 189]. These latter investigations are most readily applicable to the industrial scale fabrication of OE devices. In this final section, we will discuss the progress made towards transitioning the solution processable electro- active ink and tailored morphology innovations discussed in previous sections through these various different scales of complete device printing fabrication.

4.2. Printed OPV devices at scale

OPV devices have been the focus of intense research for the past two decades as a next generation power source due to their flexibility, light weight and simple fabrication advan- tages. While improvements in OPV device performance have attracted significant attention, the often stated advantage of solution processable materials that can be dissolved in com- mon solvents and thus can be manufactured by eco-friendly and scalable printing or coating technologies is commonly overlooked [190]. In recent years an increasing amount of attention has turned towards printable fabrication of OPV devices as the performance of materials reaches values at which they would be economic at large manufacturing scales and new innovations are developed that allow translation of material nanostructure to the large area printing equipment [191]. Initial efforts focused on translating the technology through small scale techniques such as inkjet printing. These efforts produced many insights into new difficulties in con- trolling material morphology and structure-function relation- ships in the new fluid deposition regimes. Across many years the nanoscale structure of the electroactive donor and acceptor materials has been advanced using the concepts discussed earlier with tailored material design, nanoparticle blended inks and thermodynamic treatments that are compatible with printing. This has allowed direct translation to the inkjet deposition of highly functional OPV devices, which have reached efficiencies of up to 10%, approaching the laboratory performance of these same materials [158, 192–195]. As such, here we will focus on reviewing recent efforts to translate these controlled nanostructures through to the intermediate and R2R scales.

In transitioning to the large area fabrication arena, the consumption of materials increases substantially which pro- vides a new economic restriction on the potential electroactive materials that can be pursued. Materials with simple synthetic procedures that can be cheaply upscaled are a fundamental requirement. This restriction limits many of the sophisticated ink structure innovations, resulting in almost all efforts to print OPVs at large scale employing P3HT as the donor polymer and functionalized fullerenes as the acceptor [86]. Galagan *et al* examined scaling up OPV fabrication in 2011 when they removed the ITO-glass substrate from device design, replacing it with a combination of a flexographically printed Ag grid and highly conductive PEDOT:PSS layer. Control of the

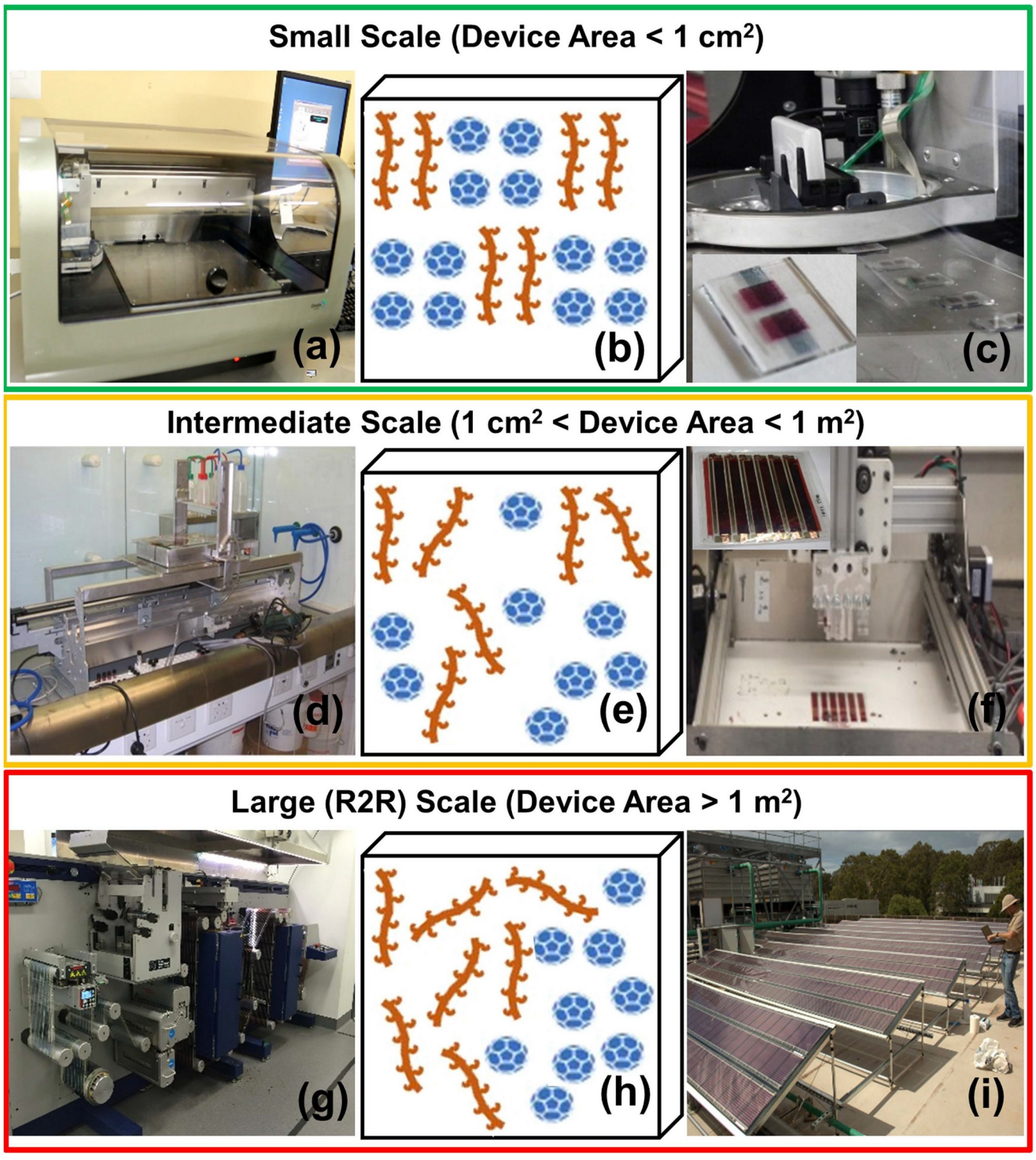

Figure 6. The three scales at which printing fabrication of OE devices has been demonstrated. Photographs show equipment for (a) small scale (benchtop inkjet printer), (c) intermediate scale (benchtop coater) and (e) large (R2R) scale (roll-to-roll coating machine). The nanoscale morphology obtained through fabrication at each scale is schematically shown as (b) highly ordered for small scale, (e) long range order for intermediate scale, and (c) highly disordered for large scale. Photographs of the typical devices prepared at each scale are also shown for (c) small scale (organic transistors with an active area of 100 mm^2), (f) intermediate scale (biosensor devices with an active area of 100 cm^2) and
(i) R2R scale (photovoltaic cells with an active area of 100 m^2).

temperature during deposition created a highly crystalline PEDOT layer and an intimately blended active layer with high carrier mobility, leading to devices with an area of 4 cm^2 which exhibited power conversion efficiencies of 1.9%, comparable

to the 2.8% observed lab based devices [196]. Voight *et al* also examined upscaled fabrication techniques, depositing PEDOT; PSS and nanostructured TiO_x charge selective contacts with a P3HT: $PC_{61}BM$ active area using gravure printing. An

efficiency of 0.6% was measured for a device with an active area of 4.5 mm^2 due to an inability to control the active layer thickness, phase segregation or the crystallinity and band gap of the electron transporting layer. However, a substantial por- tion of the device was printed using R2R compatible equip- ment. These efforts have been further developed by other groups who deposited the P3HT:PC_{61}BM active layer using R2R slot-die coating, using heated control of the head to induce a favourable active layer morphology and a solvent pretreatment of the electrode to engineer good wettability and roughness matching at the device interlayers. Such approaches produced power conversion efficiencies of 2.9% for a 1.1 cm^2 device [197], 2.3% for a 5 cm^2 device [198] and 0.8% for a 110 cm^2 device [199]. Xie *et al* subsequently trialled the pre- formed blended nanoparticle ink approach with different active layers (P3HT:PC_{61}BM, PDPP5T-2:PC_{71}BM and PTB7:PNDI-T10), fabricating the electroactive organic layers using slot-die coating with the nanostructured inks. These efforts showed increasing success, transitioning from 3.8% with the P3HT donor to an impressive 7.5% with the low band gap PTB7 polymer [160, 174, 175]. These results indicate that the nanostructure innovations developed on the small scale through ink and morphology control mechanisms can indeed be scaled to larger sizes and maintain high device performance.

The next stage of the upscaling fabrication evolution was to replace the anode lab-based glass anode structures with R2R compatible electrodes. This can be done by simply replacing ITO-glass with ITO-plastic (PET), with multiple groups demonstrating the printing of solution based OE materials onto flexible ITO-PET film, leaving only the ther- mally evaporated top electrode produced from a technique that is difficult to upscale [148, 198, 200]. This approach was explored by multiple groups, and although there was no additional nanoscience employed, it was demonstrated that the OPV device fabrication could transition to the full R2R regime with impressive power conversion efficiencies demonstrated for P3HT:PC_{61}BM (1.2%–3.1% for active areas of 0.25–156 cm^2) [201] and P3HT:ICBA (3.1%–3.2%, active area 0.25 cm^2) [200, 202]. Lucera *et al* then employed a clever processing technique to induce nanoscale patterning into devices prepared with R2R printing methods. Instead of relying on the printing process to set the geometric resolution across a 2D film, which is limited to ~65% coverage of geometric active area due to intrinsic poor resolution, they employed a femtosecond laser scribing system to provide customized nanomachining of the electroactive layers. By ablating with ultrafast laser pulses a sharp break can be placed between neighbouring cells that is of the order of hundreds of nanometres. Furthermore, the OPV stack can be selectively etched whilst leaving behind the bottom electrode, thus creating a nanostructure that is series connected but shows an active layer coverage of 98% of the 2D area. Using this nanoengineering fabrication, these authors were able to demonstrate advancement of R2R OPVs with controlled nanostructure in the electroactive inks and an induced nano- pattern to maximize electrical output, leading to 98 cm^2 devices with an efficiency of 4.5% [203].

During this period, the research group of Krebs *et al* at Denmark Technical University (DTU) produced a number of key breakthroughs in the large area fabrication space. Their infinityPV technology [181], which employs a custom developed printed Ag nanowire grid to maximize the surface area for electrical conductivity but minimize required elec- trode thickness to optimise light transmission to over 95%, has produced a number of breakthroughs in the fully printed ITO-free large area printed device research. This technology has demonstrated a number of benchmarks, creating 2% efficient devices with an active area of 40 cm^2 that charged lithium ion batteries to power a white LED flashlight [204], right through to a 250 m^2 installation with a peak power output of 1.35 kW_p [205]. This group also developed an impressive 9-layer tandem solar cell by creating a customized optoelectronic probe to examine each individual layer junc- tion and measure the charge carrier transport across these interfaces. By utilizing the insights measured at the buried
nanometer interfaces in these tandem polymer solar cells, they were able to identify several efficiency limiting printing/ coating defects arising from the nanoscale material structure and open up new opportunities for this printed OPV tech-
nology to surpass the single junction solar cell efficiency limit [206]. The full list of progress and innovations developed by this DTU group is outlined in over 200 papers published since 2011 and cannot be succinctly summarized here, but was recently reviewed in a separate article [182].

At the University of Newcastle, our team then introduced sputter coated electrodes on the R2R scale and utilized a bot- tom electrode of a printed Ag grid and solid PEDOT:PSS layer to produce devices that were entirely fabricated on the R2R scale [207]. This required an engineering of the 10 nm region in the interface between active layer and electron extracting electrode in order to establish this procedure. Initial sputtering of devices showed poor performance, which had been seen across other technologies and attributed to damage of the soft electroactive inks from the high energy sputtering particles. By performing x-ray photoelectron spectroscopy depth profiling analysis to reveal the active film morphology, nanoscale resolution of the vertical morphology distribution was revealed for the first time. This data revealed the presence of a 5–6 nm insulating oxide layer generated at the cathode interface for all sputtered samples that was not present in the traditionally prepared lab based devices. Rigorous adjustment of the oxygen level in the sputtering chamber prior to aluminium cathode deposition was found to modulate this buried interfacial layer, and indeed remove it entirely under optimised conditions to demonstrate the first ever fully R2R prepared devices with an aluminium cathode. Test modules fabricated with the new interface engineering technique revealed efficiencies of 2.2% with an active area of 13 cm^2 [208]. This stack with its opti- mized nanoscale morphology was subsequently upscaled to a 150 m^2 1 kW_p test commercial installation on a rooftop of CHEP Australia (figure 7), demonstrating the ability to trans-lation controlled nanostructure in electroactive inks from the laboratory to the large scale with only minor losses in power outputs for OPV technology [209].

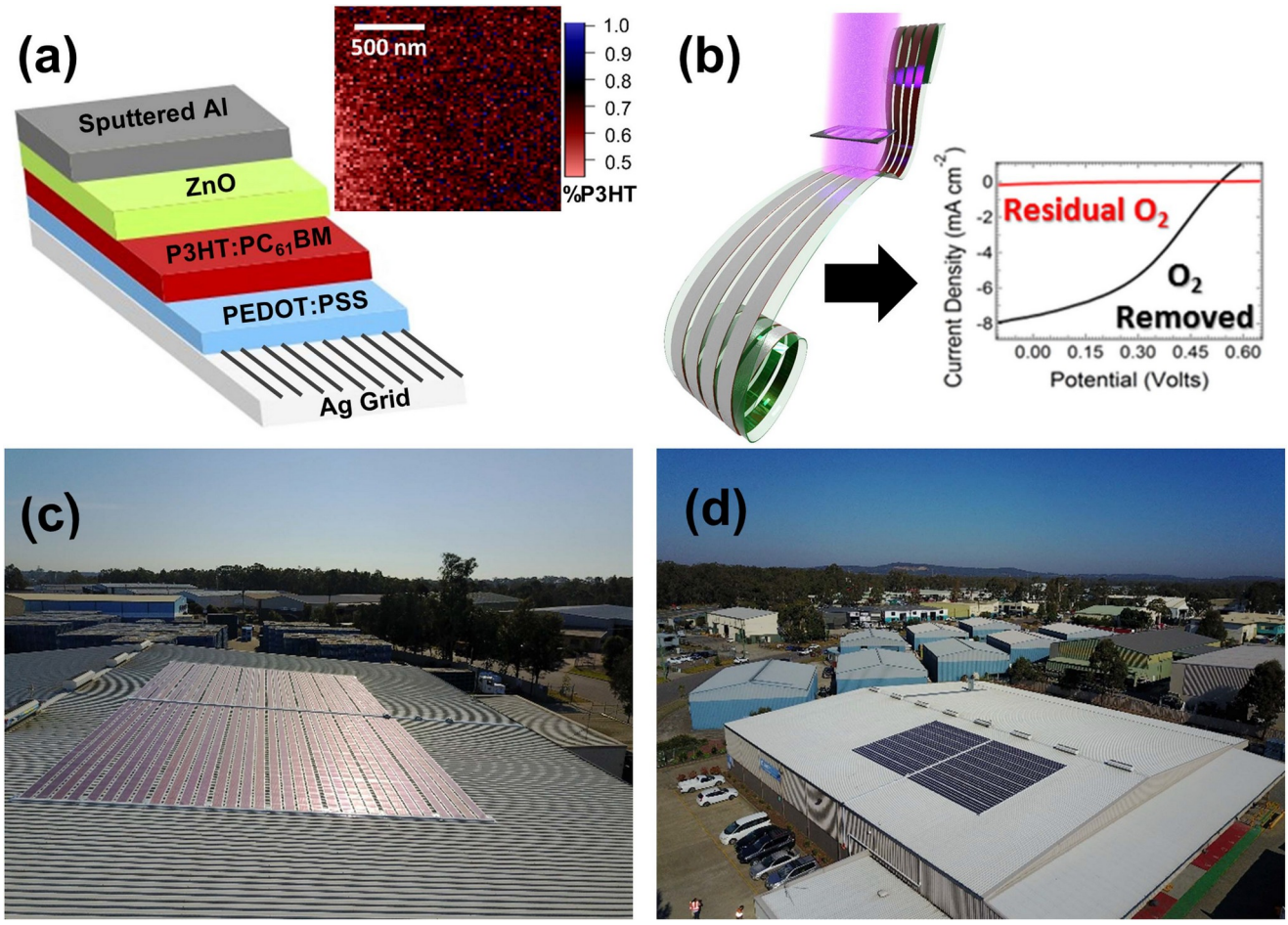

Figure 7. The schematic structure for OPV devices prepared with a sputtered aluminium cathode. The inset shows a STXM image showing molecularly blended donor–acceptor active layer morphology on a size scale below 30 nm. (b) Schematic images of the sputtered cathode and *J–V* data revealing the effect of nanoengineering the interfacial oxide layer at the cathode. (c) and (d) Images from a recent 150 m^2 commercial installation of roll-to-roll fabricated photovoltaic devices fabricated using the structure and conditions from (a) and (b) at the University of Newcastle.

4.3. Organic transistors

With the exception of OLEDs, which have been integrated into commercial products for several years now, OTFTs are the most mature of OE devices. OTFTs can be defined broadly as transistors which incorporate an organic semi- conducting material connecting their source and drain elec- trodes, although many OTFTs also incorporate organic dielectric layers and electrodes. OTFTs can be further cate- gorised according to the mechanism by which current flowing between their source and drain electrodes is modulated; common categories include organic field-effect transistors (OFETs), electrolyte-gated organic field effect transistors (EGOFETs), water-gated organic field-effect transistors (WGOFETs) and organic electrochemical transistors (OECTs). Indeed, the research laboratories of several multi- national technology companies have been publishing the results of their research and development of the field at var- ious times over the last two decades [210–212]. However, in this arena we note that the implementation of R2R fabrication for OTFTs has not yet been realised to the same extent as with OPV devices [213]. This imbalance can be attributed to the

fact that OTFT fabrication requires high device density and fine resolution of features over device size and thereby requires more sophistication in the printing techniques available.

Sirringhaus, Friend *et al* were amongst the pioneers in printing for OTFT fabrication during the early stages of the OE devices research boom. In 2000 and 2001, OTFTs fea- turing source, drain and gate electrodes inkjet-printed from a suspension of the commonly-used conducting polymer PEDOT:PSS with poly(9,9-dioctylfluoreneco-bithiophene) (F8T2) employed as a solution processed (spin-coated) semiconductor material were demonstrated [214, 215]. These materials were used to create impressive sub-nanometer channel widths by modifying the electroactive ink surface with a CF_4 plasma treatment. This tuned the surface energy of neighbouring printed droplets such that the defined channel between them was able to be deposited in a highly controlled fashion through the hydrophilicity of the ink, inducing nanoscale morphology into the semiconducting layer of the transistor [216]. These nanoscale channels created printed transistor devices where the response speed was tailored to be two orders of magnitude faster than any previous organic

transistor due to the nanostructured channel Further work in 2003 reported another novel method for defining the source– drain channel of an OTFT which combined inkjet printing and solid-state embossing in the fabrication of both ‘planar’ (conventional) and ‘vertical’ (in which the two electrodes are positioned one above the other) source–drain channels. Importantly, in the case of the vertical channel devices, sub-micron channel lengths were achieved in a highly controlled and reproducible fashion leading to organic transistors that could for the first time approach feature sizes achievable in organic devices.

Frisbie *et al* have also shown impressive outputs in the printed transistor space. In 2008 they reported the devel- opment of printable OTFTs which exhibited low-voltage operation due to the inclusion of a self-assembling ionic liquid in the dielectric layer which created a high degree of polarizability [217]. The triblock copolymer, poly (styrene-block-ethylene oxide-block-styrene) (PS-PEO-PS) was combined with 1-ethyl-3-methylimidazolium bis(tri-fluoromethylsulfonyl)imide ([EMIM][TFSI]) and printed using an aerosol jet method in order to produce a highly ordered nanostructured dielectric with a high dielectric constant. The introduction of this nanoscale ordering through the solvent coadditive createdtransistors that exhibited ambipolar operation and average charge carrier mobility values up to 50 cm^2 V^{-1} s^{-1}, orders of magnitude higher than other polymer semiconductor devices due to an enhanced field effect.

The development of printable sensors fabricated from organic transistors as the signal detection and amplifying ele- ment has been another area of increasing research interest in recent years. The group of Someya *et al* has been a leader in developing flexible, stretchable organic transistor devices pri- marily for pressure sensors. These devices have been created with a view towards developing ‘electronic skin’ for wearable textile applications (figure 8). In an early publication from 2007, they first reported the use of inkjet printing in the fab- rication of a large-area array of MEMS sensors and OTFTs [219], following this up with several reports of increasing integration of printing in their fabrication procedures for matrices of sensors and transistors [220–222]. These sensors utilise the ability to print highly conductive nanostructured Ag inks, which are incorporated into a soft and stretchable insu-lating matrix that can only be formed through solution based fabrication techniques. When the matrix is compressed the silver particles form a conducting network to switch the tran- sistor into an on state. The loading of the conducting silver particles can be systematically varied to tune both the electrical conductivity and mechanical strength of the printed materials, allowing the sensitivity of the sensors to be systematically tuned based upon the specific nanostructure of the conducting matrix to mimic that of differing areas of the human body [223]. Similar types of organic sensors reported in the func- tional printing literature include strain sensors [224], pressure sensors for explosives detonation [225], and sensing of light by photodiodes that is produced by bending or straining an external optical signal carrying element [226, 227].

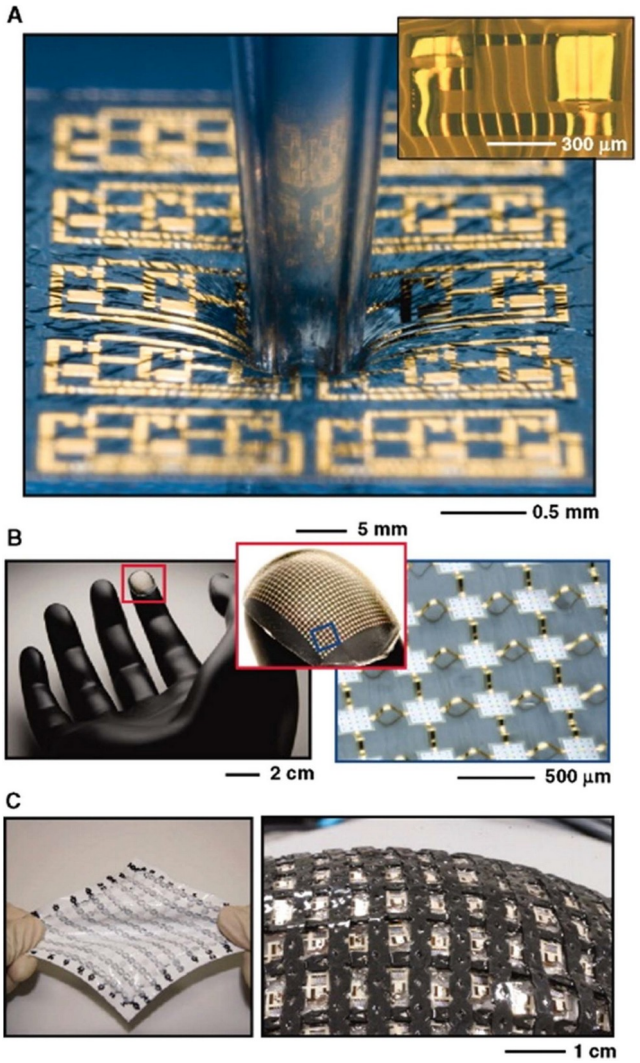

Figure 8. Examples of flexible electronics, including (a) a stretchable silicon transistor circuit compressed by a capillary tube, (b) stretchable transistor circuit molded onto a model of a fingertip, and (c) and array of organic transistors deposited onto a flexible PDMS substrate and connected by elastic conductors. Figure was reproduced with permission from [218]. Copyright 2010 by the American Association for the Advancement of Science.

Printing organic semiconductors from liquid phase (either a polymer-based solution or nanoparticulate disper- sion) historically produces films which are amorphous or have relatively small crystalline domains and consequently exhibit poor mobility values in comparison with those fabricated from highly crystalline inorganic semiconductors [12]. However, developments in functional printing have pro- gressed to now allow highly crystalline materials to be deposited by utilizing clever nanostructuring approaches. Hasegawa *et al* first demonstrated a method in 2011 which has the potential to combine the advantages of printing fab- rication with the performance of semiconductor films of high morphological quality [139]. By first inkjet printing a non- solvent, followed by a solution of the functional material (in a technique dubbed double-shot inkjet printing), a slow crys- tallisation is induced at the nanostructured interface of the two

solvents as they evaporate, forming highly crystalline or single-crystal films with significantly higher charge carrier mobilities than had been previously possible in organic materials. In this case, crystals of the semiconductor 2,7- dioctyl[1]benzothieno[3,2-b][1] benzothiophene (C_8-BTBT) were printed with mobility values up to 16.4 $cm^2 V^{-1} s^{-1}$ obtained from the resulting OTFTs. In recent years, a variety of related advances have been reported by several groups. In 2017 Conti *et al* demonstrated all inkjet-printed OFETs with low-voltage operation and mobility values up to 1 $cm^2 V^{-1} s^{-1}$ from the commonly used soluble organic semiconductor 6,13-bis(triisopropylsilylethynyl) pentacene (TIPS pentacene) [135], whilst Tokito *et al* reported the use of inkjet printing in combination with a computer-controlled dispensing system to fabricate high performance OTFTs on ultra-thin (1 μm thick) parylene-C substrates [228]. The high electrical performance of these devices is fundamentally dependent on the nanos- tructured interface formed between orthogonal solvent con- trolling the highly directional growth of the active layers in the semiconducting channel.

Fraboni *et al* have adapted the approach described above, pioneering the use of single crystal OE materials as the semi- conducting component of thin film-transistors for direct sensing of ionizing radiation [229, 230]. Through a series of seminal papers they have demonstrated the incorporation of single crystal organic semiconductors such as TIPS-pentacene and rubrene [231, 232], anthradithiophenes [233] and 4-hydroxycyanobenzene (4HCB) [229] into organic thin film transistors. These transistor devices subsequently exhibited impressive charge carrier mobility of up to 2.5 $cm^2 V^{-1} s^{-1}$ and radiation sensitivities of 120 nC Gy^{-1} at low operating voltages of 1–10 V. These studies have been accompanied by attempts to replace the organic semiconducting crystals with organic semiconducting polymers such as poly(triarylamines), although the precision nanocrystalline structure is lost in these semi-conducting polymers and the carrier mobilities are lower, requiring much higher operating voltages (100 V) [234–236]. To circumvent this limited mobility, indirect sensitization of radiation has also been studied, by combining a P3HT:PC_{61}BM organic photodiode with phosphor scintillators terbium and europium-doped gadolinium oxide (GOS:Tb, GOS:Eu). Agos- tinelli *et al* incorporated GOS:Tb into a P3HT: PC_{61}BM device prepared using spin coating methods and showed a photo- current response of 300 nA at a dose rate of 8 mGs^{-1} [237]. However, Büchele *et al* employed targeted nanoengineering of the OE materials to demonstrate enormous sensitivity improvements and fabricate devices with outputs rivalling commercial x-ray detectors. This was achieved by first creating nanoparticles of the x-ray absorbing scintillator and subse- quently blending these intimately with the organic photodiode. This significantly optimised the light and energy transfer path- ways by bringing all active components within 10–50 nm of each other, demonstrating impressive sensitivities of 75 nC Gy^{-1} mm^{-2} for GOS:Tb inside a P3HT:PC_{61}BM organic photodiode layer [238], and 1712 mC Gy^{-1} cm^{-3} for bismuth oxide scintillator particles inside the same photodiode structure [239]. Excitingly, this approach has now been translated to printing fabrication techniques, with creation of a transistor

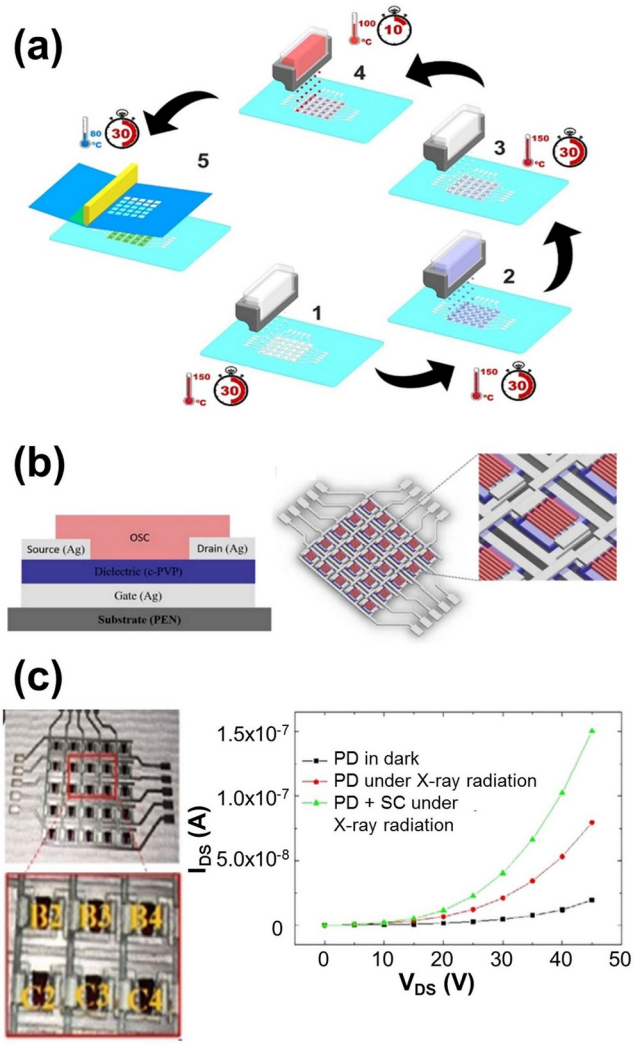

Figure 9. (a) A schematic representation of the printing procedure for preparing multilayer radiation sensors composed of (1) a Ag electrode; (2) a dielectric layer (PVP); (3) Ag source and drain electrodes; (d) a semiconducting polymer layer; (5) the scintillator ink. (b) A schematic image of the layer structure for both the individual radiation sensors and a 5 × 5 array prepared for imaging. (c) Photographs of the devices and *I*–*V* curves of one of the single photodiodes (PDs) present in the array in dark (black curve) and under x-ray radiation with (green curve) and without (red curve) the scintillator (SC) film. Figure was reproduced with permission from [186]. Copyright 2018 by the American Chemical Society.

structure composed of a commercial p-type semiconductor and PVP dielectric being successfully inkjet-printed (figure 9) [186]. Finally, much like for OPVs, the innovations creating specific nanostructured materials that induce high device performance are being translated to larger scale fabrication equipment. The group of Sandberg *et al* has presented a different take on R2R OTFT fabrication which involves laminating two individually-printed substrates together at the semiconductor-dielectric interface [188]. This physical lamination process has the advantage of allowing the printable fabrication of materials which would not otherwise be sui- table for direct liquid phase deposition due to incompat- ibilities in orthogonality of solvents or surface energy issues.

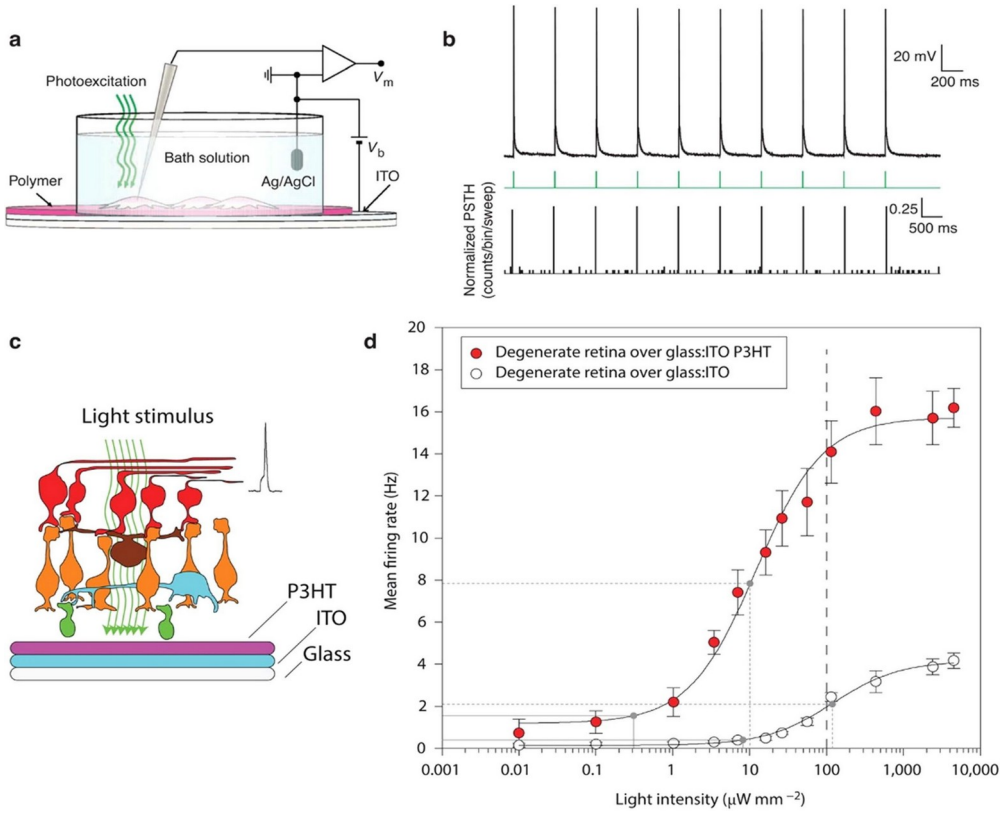

Figure 10. (a) Schematic illustration of a neuron grown on top of a nanopatterned P3HT organic semiconducting electrode. (b) Action potential responses after light pulse stimulations (green). (c) Illustration of the restoration of light response in the structure of an eye using the interface between patterned P3HT and neurons. Figure reproduced with permission from [11]. Copyright 2012 by Springer Nature.

By adopting the lamination approach, the interface of joining can have the surface energy tuned through functionalisation, with this interfacial nanoscale region then responsible for adhering the device together through strong intermolecular forces. In the high-throughput R2R printing space, Krebs' group at DTU, Denmark has demonstrated the use of a variety of R2R techniques to fabricate organic transistors on a large scale. The methods of printing employed were flexographic printing for the source and drain electrodes, slot-die coating for the semiconductor and dielectric layers and screen printing for the gate electrode [156].

4.4. Printed biofunctional sensors

As discussed in the earlier introduction, organic bioelectronics involves coupling OE materials and devices directly with biological systems to selectively sense, record, and monitor different signals and physiological states, as well as convert relevant parameters into electronic readout for further proces- sing and decision making [11]. There are many ways that this can be done, but perhaps the most common has been to incorporate biofunctional molecules into the semiconductor or gate component of an electrochemical transistor. These devices operate by movement of ions through the dielectric to dope the semiconducting channel instead of an electric field, thus making them highly compatible with biological systems, which transfer signals through ionic conduction [153]. The char- acteristics of an OECT can be tailored by changing the channel

geometry, which can be performed with hundred nanometer resolution in printing fabrication. The drain current, and thus the transconductance, is directly modified by the channel width, thickness and length [15]. For thicker polymer films the ionic transport limits the speed of the transistor switching, but a relatively higher transconductance can be obtained. The elec- trochemical transistor has been used to incorporate a range of biorecognition elements and create printed biosensors. In this area, Malliaras *et al* demonstrated the screen-printing of an enzymatic transistor-based sensor designed to measure the levels of glucose and lactose in sweat [187]. More recently, Malliaras was involved in a collaborative study which reported the successful fabrication of enzymatic inkjet-printed ethanol sensors for breath-testing applications [240]. Because the organic semiconductors are so susceptible to small changes in
ionic dopant content, they act as voltage transducers with low bias voltages (~1 to 10 V) and very high sensitivity which can be modulated by controlling the nanostructure of the dielectric using the solvent washing technique described in the previous
section. At the University of Newcastle, we have previously demonstrated printable organic biosensors based on both an enzyme-containing OTFT for glucose sensing [123], and a crown-ether-modified chemiresistor for sodium ion sensing
[70] that operate on the same principles. The group of Borto- lotti has demonstrated the successful fabrication of a tumour necrosis factor alpha (TNFα) sensors using anti-TNFα as a recognition element grafted on to the gate electrode of the

Figure 11. (a) A large area ‘solar city’ exhibited at Pacprint 2017 in Melbourne (Australia) to demonstrate printed solar cell technology at scale. (b) Radiation detectors printed at scale being investigated with a clinical phantom on a medical linear accelerator, and (c) an expanded view of the flexible printed radiation sensors shown in (b).

transistor [241], while Magliulo *et al* demonstrated another similar type of device, this time with the recognition element (anti-C-reactive protein monoclonal antibody) bound to the semiconductor layer rather than the gate electrode [242].

For useful organic bioelectronics applications, the semi- conductor material must allow adhesion and support for biological cells to establish intimate contact with living tissue. While many organic semiconductors are found to be bio- compatible, cells will not directly adhere to all biocompatible polymers. Surfaces with electrical stimuli-responsive proper- ties such as functionalized electrodes and transistor devices are also essential for the realization of smart, highly engi- neered cell–material interfaces. Harris *et al* have shown that both nanostructured carbon and conducting polymer electro- des have shown success in promoting the growth of neuronal cells. They have demonstrated that matching the nanos- tructured electrode pattern to the cell recognition element structure provides optimal conditions for adhesion and sti- mulation of living tissue [109]. Further recent studies demonstrated that nanopatterning of organic semiconducting inks through the printing processes discussed in this article can aid in both the biocompatibility[122] and the guidance of neurite axons, which have a clear preferred orientation in nanopatterned conducting polymer arrays [59, 125]. This works reports that the nanostructuring of the organic

electrodes is critical for creating viable biointerfaces. Optical methods are another an attractive alternative to direct elec- tronic stimulation for interfacing with cells, primarily due to the high spatial and/or temporal resolution that can be achieved by light [11]. Zangoli *et al* have shown that nano-particles prepared from appropriately functionalized poly- thiophenes once administered to live cells can acquire phototransduction properties under illumination, becoming photoactive sites able to absorb visible light and convert it to an electrical signal through cell membrane polarization [72]. This finding was reinforced by Feron *et al*, who recently reported both improved biocompatibility and an ability to photostimulate neurons using red, green and blue absorbing nanostructured conducting polymers. They found that the light interaction is a surface mediated capacitive mechanism, and thus requires a highly functionalized surface that must be strongly nanoengineered. The approach was taken a step further by *et al*, who fabricated an entire printed biocompa- tible OPV device with integrated wireless electrical power supply units as an organic bioelectronic interface electrode that can be operated under illumination with near-infrared light and successfully stimulate PC12 neuronal cells to grow. The tunable spectral response, low voltage operation and flexibility have been used to employ OPV devices as retinal implants (figure 10). Ghezzi *et al* placed P3HT

nanostructured electrodes into rat retinas in an effort to restore light sensitivity to the tissue in a spatially resolved fashion that arises from the patterning of the printable P3HT layer [243]. After photostimulation at 532 nm, neuronal activity was observed with a firing rate that was strongly dependent on light intensity.

5. The outlook for biocompatible OE devices at large scale

Opportunities for the utilization of OE materials in innovative applications are continuing to rapidly expand. Such oppor- tunities are driven by the unique electroactive functionality and inherent biocompatability offered by these carbon-based semiconductors. However, the transition from the laboratory space into commercial products is presently limited by an inability to fabricate devices economically at the mass man- ufacturing scale. Printing fabrication of these solution pro- cessable material components offers a direct route towards upscaled manufacture using roll-to-roll manufacture at ambient temperatures with fast and rapid patterning and device characterisation performed in continuous, high-speed processes.

Although many innovative organic technologies have been developed in the laboratory, the major restrictions on upscaling these research success stories remains an inability to translate strategies to control the precise material nanoscale into the large scale fabrication arena, where the length scales rapidly increase. Understanding the material properties and developing new structure-function relationships for organic materials through advanced characterisation techniques is a critical next step in progressing this field. Despite the limited progress, there are promising new materials fabrication routes, such as the creation of nanostructured inks, that are showing early promise in scaling a range of solar cell and sensor devices to the large scale. There have been success stories, particularly in the arena of large printed photovoltaic arrays, R2R printing of transistor structures and recent inno- vations in mechanical and radiation sensors that provide an insight into exciting new opportunities for OE devices (figure 11). In order to realize this potential, facilities must be developed that simultaneously conduct research across a range of fabrication scales to develop new laboratory inno- vations in conjunction with large area printing that provides an active feedback loop to the laboratory development path- way. There is still much more work to be done to allow these exciting materials to reach their full potential in emerging research fields including bioelectronics, wearable electronics and renewable energy generation. However, the evidence is now clear that the transition of OE devices to commercial products is realizable, and the innovations of today are only a small step away from becoming the reality of the technolo- gical world in which we live.

Acknowledgments

This work was performed in part at the Materials node of the Australian National Fabrication Facility, a company estab- lished under the National Collaborative Research Infra- structure Strategy to provide nano and microfabrication facilities for Australia's researchers. This research used resources of the Advanced Light Source, which is a DOE Office of Science User Facility under contract no. DE- AC02–05CH11231. We acknowledge travel funding pro- vided by the International Synchrotron Access Program (ISAP) managed by the Australian Synchrotron, part of ANSTO, and funded by the Australian Government. The authors thank Professor Paul Dastoor for several useful dis- cussions and insights. The authors have confirmed that any identifiable participants in this study have given their consent for publication.

ORCID iDs

Matthew J Griffith https://orcid.org/0000-0002-5761-1860

References

Q2

[1] Kamyshny A and Magdassi S 2014 *Small* 10 3515
[2] Anthony J E 2014 *Nat. Mater.* 13 773
[3] *Consumer Electronics Market by Product—Global Industry Perspective* (Zion Market Research) 2018
[4] Hwang K, Jung Y-S, Heo Y-J, Scholes F H, Watkins S E, Subbiah J, Jones D J, Kim D-Y and Vak D 2015 *Adv. Mater.* 27 1241
[5] Lin Q, Nagiri R C R, Burn P L and Meredith P 2016 *Adv. Opt. Mater.* 5 1600819
[6] Eggenhuisen T M *et al* 2015 *J. Mater. Chem.* A 3 7255
[7] Seyler H, Haid S, Kwon T-H, Jones D J, Bäuerle P, Holmes A B and Wong W W H 2013 *Aust. J. Chem.* 66 151
[8] Lipomi D J and Bao Z 2017 *MRS Bull.* 42 93
[9] Sunahara K, Griffith M J, Uchiyama T, Wagner P, Officer D L, Wallace G G, Mozer A J and Mori S 2013 *ACS Appl. Mater. Interfaces* 5 10824
[10] Ameri M *et al* 2019 *ACS Appl. Mater. Interfaces* Accepted
[11] Simon D T, Gabrielsson E O, Tybrandt K and Berggren M 2016 *Chem. Rev.* 116 13009
[12] Li J *et al* 2012 *Sci. Rep.* 2 754
[13] Ho S, Liu S, Chen Y and So F 2015 *J. Photonics Energy* 5 057611
[14] Volz D 2016 *J. Photonics Energy* 6 020201
[15] Rivnay J, Inal S, Salleo A, Owens R M, Berggren M and Malliaras G G 2018 *Nat. Rev. Mater.* 3 17086
[16] Liu D and Miao Q 2018 *Mater. Chem. Front.* 2 11
[17] Elumalai N K and Uddin A 2016 *Energy Environ. Sci.* 9 391
[18] Lu L, Zheng T, Wu Q, Schneider A M, Zhao D and Yu L 2015 *Chem. Rev.* 15 12666
[19] Lee M Y, Lee H R, Park C H, Han S G and Oh J H 2018 *Acc. Chem. Res.* 51 2829
[20] Chen D and Pei Q 2017 *Chem. Rev.* 117 11239
[21] Feron K, Lim R, Sherwood C, Keynes A, Brichta A and Dastoor P C 2018 *Int. J. Mol. Sci.* 19
[22] Jeevanandam J, Barhoum A, Chan Y S, Dufresne A and Danquah M K 2018 *Beilstein J. Nanotech.* 9 1050

[23] Yin Y and Talapin D 2013 *Chem. Soc. Rev.* 42 2484
[24] Gleiter H 2000 *Acta Mater.* 48 1
[25] Li Z, Xu X, Zhang W, Meng X, Ma W, Yartsev A, Inganas O, Andersson M R, Janssen R A and Wang E 2016 *J. Am. Chem. Soc.* 138 10935
[26] Griffith M J, Cooling N A, Vaughan B, Elkington D C, Hart A S, Lyons A G, Qureshi S, Belcher W J and Dastoor P C 2016 *IEEE J. Sel. Top. Quantum Electron.* 22 1
[27] Martin C R 2002 *Acc. Chem. Res.* 28 61
[28] Ghosh S, Maiyalagan T and Basu R N 2016 *Nanoscale* 8 6921
[29] Yin Z and Zheng Q 2012 *Adv. Energy. Mater.* 2 179
[30] Nguyen D N and Yoon H 2016 *Polymers* 8
[31] Tong M, Coates N E, Moses D, Heeger A J, Beaupré S and Leclerc M 2010 *Phys. Rev.* B 81 125210
[32] Riede M, Mueller T, Tress W, Schueppel R and Leo K 2008 *Nanotechnology* 19 424001
[33] Vandewal K *et al* 2014 *Nat. Mater.* 13 63
[34] Qin T, Zajaczkowski W, Pisula W, Baumgarten M, Chen M, Gao M, Wilson G, Easton C D, Müllen K and Watkins S E 2014 *J. Am. Chem. Soc.* 136
[35] Griffith M J and Mozer A J 2011 Porphyrin based dye sensitized solar cells *Solar Cells: Dye-Senstized Devices* ed L Kosyachenko (Rijeka: InTech)
[36] Ikeuchi T, Nomoto H, Masaki N, Griffith M J, Mori S and Kimura M 2014 *Chem. Commun.* 1941
[37] Mozer A J *et al* 2009 *J. Am. Chem. Soc.* 131 15621
[38] Griffith M J, Sunahara K, Wagner P, Wagner K, Wallace G G, Officer D L, Furube A, Katoh R, Mori S and Mozer A J 2012 *Chem. Commun.* 48 4145
[39] Begum F, Ferguson J, McKenna K, McNamara L E, Hammer N I and Rathnayake H 2013 *New J. Chem.* 37 1
[40] Wallace J U, Young R H, Tang C W and Chen S H 2007 *Appl. Phys. Lett.* 91 152104
[41] Mozer A J, Sariciftci N S, Pivrikas A, Österbacka R, Juška G, Brassat L and Bässler H 2005 *Phys. Rev.* B 71
[42] Zheng C, Xu X, He F, Li L, Wu B, Yu G and Liu Y 2010 *Langmuir* 26 16730
[43] Liao H-C, Ho C-C, Chang C-Y, Jao M-H, Darling S B and Su W-F 2013 *Mater. Today* 16 326
[44] Ji G, Zhao W, Wei J, Yan L and Han Y 2019 *J. Mater. Chem.* A 7 212
[45] Badrou Aïch R, Zou Y, Leclerc M and Tao Y 2010 *Org. Electron.* 11 1053
[46] Zhang F, Jespersen K G, Björström C, Svensson M, Andersson M R, Sundström V, Magnusson K, Moons E, Yartsev A and Inganäs O 2006 *Adv. Funct. Mater.* 16 667
[47] Clarke T M and Durrant J R 2010 *Chem. Rev.* 110 6736
[48] Pivrikas A, Neugebauer H and Sariciftci N S 2010 *IEEE J. Sel. Top. Quantum Electron.* 16 1746
[49] Armin A, Juska G, Philippa B W, Burn P L, Meredith P, White R D and Pivrikas A 2013 *Adv. Energy Mater.* 3 321
[50] Maurano A *et al* 2010 *Adv. Mater.* 22 4987
[51] Clarke T M, Lungenschmied C, Peet J, Drolet N and Mozer A J 2015 *J. Phys. Chem.* C 119 7016
[52] Hansson R *et al* 2015 *J. Mater. Chem.* A 3 6970
[53] Lin P and Yan F 2012 *Adv. Mater.* 24 34
[54] Choi S, Lee H, Ghaffari R, Hyeon T and Kim D-H 2016 *Adv. Mater.* 28 4203
[55] Lee S S and Loo Y L 2010 *Annu. Rev. Chem. Biomol. Eng.* 1 59
[56] Huang Y, Su N, Zhang X, Zhao J, Li H, Liu X and Zhang H 2014 *Polym. Compos.* 35 1858
[57] Zhang X, Huang Y, Huang X, Huang C and Li H 2016 *Polym. Compos.* 37 462
[58] Mabrook M F, Pearson C and Petty M C 2006 *Sensors Actuators* B 115 547
[59] Gomez N, Lee J Y, Nickels J D and Schmidt C E 2007 *Adv. Funct. Mater.* 17 1645

[60] Huang J, Virji S, Weiller B H and Kaner R B 2003 *J. Am. Chem. Soc.* 125 314
[61] Wang H J, Ji L W, Li D F and Wang J Y 2008 *J. Phys. Chem.* B 112 2671
[62] Tang Z, Wu J, Zheng M, Tang Q, Liu Q, Lin J and Wang J 2012 *RSC Adv* 2
[63] Bidez P R, Li S, MacDiarmid A G, Venancio E C, Wei Y and Lelkes P I 2012 *J. Biomater. Sci* 17 199
[64] Baker C O, Huang X, Nelson W and Kaner R B 2017 *Chem. Soc. Rev.* 46 1510
[65] Baran D *et al* 2017 *Nat. Mater.* 16 363
[66] Wadsworth A *et al* 2018 *Adv. Energy Mater.* 8
[67] Goh C, Kline R J, McGehee M D, Kadnikova E N and Fréchet J M J 2005 *Appl. Phys. Lett.* 86
[68] Kim H J, Lee M Y, Kim J S, Kim J H, Yu H, Yun H, Liao K, Kim T S, Oh J H and Kim B J 2017 *ACS Appl. Mater. Interfaces* 9 14120
[69] Nam S, Kim J, Lee H, Kim H, Ha C S and Kim Y 2012 *ACS Appl. Mater. Interfaces* 4 1281
[70] Holmes N P, Elkington D C, Walters J, Nicholson L M, Capozza M, Magno M H R, Vijayarajan S, Zhou X, Belcher W J and Dastoor P C 2018 *Med. Dev. Sens.* 1
[71] Merkle R, Gutbrod P, Reinold P, Katzmaier M, Tkachov R, Maier J and Ludwigs S 2017 *Polymer* 132 216
[72] Zangoli M, Di Maria F, Zucchetti E, Bossio C, Antognazza M R, Lanzani G, Mazzaro R, Corticelli F, Baroncini M and Barbarella G 2017 *Nanoscale* 9 9202
[73] Dou L, Liu Y, Hong Z, Li G and Yang Y 2015 *Chem. Rev.* 115 12633
[74] Brabec C J and Durrant J R 2008 *MRS Bull.* 33 670
[75] Zhuang W *et al* 2013 *J. Mater. Chem.* A 1
[76] Dou L, You J, Hong Z, Xu Z, Li G, Street R A and Yang Y 2013 *Adv. Mater.* 25 6642
[77] Liang Y, Feng D, Wu Y, Tsai S T, Li G, Ray C and Yu L 2009 *J. Am. Chem. Soc.* 131 7792
[78] Hou J, Park M-H, Zhang S, Yao Y, Chen L-M, Li J-H and Yang Y 2008 *Macromolecules* 41 6012
[79] Zhang S, Qin Y, Zhu J and Hou J 2018 *Adv. Mater.* 30 e1800868
[80] Yuan J *et al* 2019 *Joule*
[81] Kim Y J and Park C E 2016 *Nanoscale* 8 7654
[82] Sun C, Pan F, Bin H, Zhang J, Xue L, Qiu B, Wei Z, Zhang Z G and Li Y 2018 *Nat. Commun.* 9 743
[83] Semenov K N, Charykov N A, Keskinov V A, Piartman A K, Blokhin A A and Kopyrin A A 2010 *J. Chem. Eng. Data* 55 13
[84] Rossbauer S, Müller C and Anthopoulos T D 2014 *Adv. Funct. Mater.* n/a
[85] Mendaza A D, Melianas A, Rossbauer S, Backe O, Nordstierna L, Erhart P, Olsson E, Anthopoulos T D, Inganas O and Muller C 2015 *Adv. Mater.* 27 7325
[86] Cooling N A *et al* 2016 *J. Mater. Chem.* A 4 10274
[87] Lee J, Ko S-J, Seifrid M, Lee H, McDowell C, Luginbuhl B R, Karki A, Cho K, Nguyen T-Q and Bazan G C 2018 *Adv. Energy. Mater* 8
[88] Zhang L, Lin B, Ke Z, Chen J, Li W, Zhang M and Ma W 2017 *Nano Energy* 41 609
[89] Chen F X *et al* 2018 *Adv. Mater.* 30 e1803769
[90] Lin Y *et al* 2016 *J. Am. Chem. Soc.* 138 2973
[91] Huang J, Wang X, Zhang X, Niu Z, Lu Z, Jiang B, Sun Y, Zhan C and Yao J 2014 *ACS Appl. Mater. Interfaces* 6 3853
[92] Bu L, Guo X, Yu B, Qu Y, Xie Z, Yan D, Geng Y and Wang F 2009 *J. Am. Chem. Soc.* 131 13242
[93] Zhang J L, Zhong S, Zhong J Q, Niu T C, Hu W P, Wee A T and Chen W 2015 *Nanoscale* 7 4306
[94] Singh M, Haverinen H M, Dhagat P and Jabbour G E 2009 *Adv. Mater.* 22 673

[95] Carlé J E, Andersen T R, Helgesen M, Bundgaard E, Jørgensen M and Krebs F C 2013 *Solar Energy Mater. Solar Cells* 108 126
[96] Rajan K, Roppolo I, Chiappone A, Bocchini S, Perrone D and Chiolerio A 2016 *Nanotechnol. Sci. Appl.* 9 1
[97] Espinosa N, Hösel M, Angmo D and Krebs F C 2012 *Energy Environ. Sci.* 5 5117
[98] Ding Z, Stoichkov V, Horie M, Brousseau E and Kettle J 2016 *Solar Energy Mater. Solar Cells* 157 305
[99] Kim S, Yun T G, Kang C, Son M-J, Kang J-G, Kim I-H, Lee H-J, An C-H and Hwang B 2018 *Mater. Des.* 151 1
[100] Finn D J, Lotya M and Coleman J N 2015 *ACS Appl. Mater. Interfaces* 7 9254
[101] Stewart I E, Kim M J and Wiley B J 2017 *ACS Appl. Mater. Interfaces* 9 1870
[102] Hwang H J and Malhotra R 2019 *ACS Appl. Mater. Interfaces* 11 3536
[103] Andersen T R *et al* 2016 *Sol. Energy Mater. Sol. Cells* 149 103
[104] Akter M, Sikder M T, Rahman M M, Ullah A, Hossain K F B, Banik S, Hosokawa T, Saito T and Kurasaki M 2018 *J. Adv. Res.* 9 1
[105] Iijima S 1991 *Nature* 354 56
[106] Novoselov K S, Geim A K, Morozov S V, Jiang D, Zhang Y, Dubonos S V, Grigorieva I V and Firsov A A 2004 *Science* 306 666
[107] Santhiago M, Correa C C, Bernardes J S, Pereira M P, Oliveira L J M, Strauss M and Bufon C C B 2017 *ACS Appl. Mater. Interfaces* 9 24365
[108] Silva T A, Moraes F C, Janegitz B C and Fatibello-Filho O 2017 *J. Nanomater.* 2017 1
[109] Harris A R and Wallace G G 2018 *Adv. Funct. Mater.* 28
[110] Niyogi S, Bekyarova E, Itkis M E, McWilliams J L, Hamon M A and Haddon R C 2006 *J. Am. Chem. Soc.* 128 7720
[111] Patil U, Lee S C, Kulkarni S, Sohn J S, Nam M S, Han S and Jun S C 2015 *Nanoscale* 7 6999
[112] Mondal S, Rana U and Malik S 2017 *J. Phys. Chem.* C 121 7573
[113] Guo X, Zheng S, Zhang G, Xiao X, Li X, Xu Y, Xue H and Pang H 2017 *Energy Storage Mater.* 9 150
[114] Serafin V, Torrente-Rodriguez R M, Gonzalez-Cortes A, Garcia de Frutos P, Sabate M, Campuzano S, Yanez-Sedeno P and Pingarron J M 2018 *Talanta* 179 131
[115] Vicentini F C, Raymundo-Pereira P A, Janegitz B C, Machado S A S and Fatibello-Filho O 2016 *Sensors Actuators* B 227 610
[116] Mendes P M 2013 *Chem. Soc. Rev.* 42 9207
[117] Liao C, Zhang M, Yao M Y, Hua T, Li L and Yan F 2015 *Adv. Mater.* 27 7493
[118] Lee J M and Yeong W Y 2016 *Adv. Healthc. Mater* 5 2856
[119] Kokkinis D, Bouville F and Studart A R 2018 *Adv. Mater.* 30 e1705808
[120] Chia H N and Wu B M 2015 *J Biol Eng* 9 4
[121] Zhang Y, Zhang F, Yan Z, Ma Q, Li X, Huang Y and Rogers J A 2017 *Nat. Rev. Mater.* 2
[122] Zhu Z, Guo S Z, Hirdler T, Eide C, Fan X, Tolar J and McAlpine M C 2018 *Adv. Mater.* 30 e1707495
[123] Elkington D, Wasson M, Belcher W, Dastoor P C and Zhou X 2015 *Appl. Phys. Lett.* 106
[124] Ihalainen P, Maattanen A and Sandler N 2015 *Int. J. Pharm.* 494 585
[125] Joo S, Kang K and Nam Y 2015 *J. Biomed. Mater. Res.* A 103 2731
[126] Hsiao Y S, Liao Y H, Chen H L, Chen P and Chen F C 2016 *ACS Appl. Mater. Interfaces* 8 9275
[127] Yin W and Dadmun M 2011 *ACS Nano* 5 4756

[128]Brabec C J, Zerza G, Cerullo G, De Silvestri S, Luzzati S, Hummelen J C and Sariciftci S 2001 *Chem. Phys. Lett.* 340 232
[129]Hoppe H and Sariciftci N S 2006 *J. Mater. Chem.* 16 45
[130]Ye L, Collins B A, Jiao X, Zhao J, Yan H and Ade H 2018 *Adv. Energy Mater.* 8
[131]He X, Collins B A, Watts B, Ade H and McNeill C R 2012 *Small* 8 1920
[132]Collins B A, Gann E, Guignard L, He X, McNeill C R and Ade H 2010 *J. Phys. Chem. Lett.* 1 3160
[133]Treat N D, Shuttle C G, Toney M F, Hawker C J and Chabinyc M L 2011 *J. Mater. Chem.* 21
[134]Graddage N, Chu T-Y, Ding H, Py C, Dadvand A and Tao Y 2016 *Org. Electron.* 29 114
*[135]*Conti S, Lai S, Cosseddu P and Bonfiglio A 2017 *Adv. Mater. Technol.* 2
[136]Chen J, Zhang L, Jiang X, Gao K, Liu F, Gong X, Chen J and Cao Y 2017 *Adv. Energy Mater.* 7
[137]Wang Y, Zhu H, Shi Z, Wang F, Zhang B, Dai S and Tan Z A 2017 *J. Mater. Chem.* A 5 2319
[138]Liu F, Ferdous S, Schaible E, Hexemer A, Church M, Ding X, Wang C and Russell T P 2015 *Adv. Mater.* 27 886
[139]Minemawari H, Yamada T, Matsui H, Tsutsumi J, Haas S, Chiba R, Kumai R and Hasegawa T 2011 *Nature* 475 364
[140]Palumbiny C M, Liu F, Russell T P, Hexemer A, Wang C and Muller-Buschbaum P 2015 *Adv. Mater.* 27 3391
[141]Rivnay J, Inal S, Collins B A, Sessolo M, Stavrinidou E, Strakosas X, Tassone C, Delongchamp D M and Malliaras G G 2016 *Nat. Commun.* 7 11287
[142]Ro H W *et al* 2016 *Energy Environ. Sci.* 9 2835
[143]Huang Y-C, Cha H-C, Chen C-Y and Tsao C-S 2016 *Solar Energy Mater. Solar Cells* 150 10
*[144]*Hösel M, Dam H F and Krebs F C 2015 *Energy Technol.* 3 293
[145]Koutsiaki C, Kaimakamis T, Zachariadis A, Papamichail A, Kamaraki C, Fachouri S, Gravalidis C, Laskarakis A and Logothetidis S 2019 *Org. Electron.* 73 231
[146]Zhang L *et al* 2018 *Adv. Mater.* 30 e1805041
[147]Park J and Rhee S 2010 *Japan. J. Appl. Phys.* 49
[148]Gu X *et al* 2017 *Adv. Energy. Mater.* 7
*[149]*Dimitrakopoulos C D and Mascaro D J 2001 *IBM J. Res. Dev.* 45 11
*[150]*Wang Z, Zhang Y, Zhang J, Wei Z and Ma W 2016 *Adv. Energy Mater.* 6
*[151]*Cha H, Park C E, Kwon S-K and An T K 2017 *Org. Electron.* 45 263
[152]Mai J, Lau T-K, Li J, Peng S-H, Hsu C-S, Jeng U S, Zeng J, Zhao N, Xiao X and Lu X 2016 *Chem. Mater.* 28 6186
*[153]*Wang N, Yang A, Fu Y, Li Y and Yan F 2019 *Acc. Chem. Res.* 52 277
[154]Afonso M, Morgado J and Alcácer L 2016 *J. Appl. Phys.* 120
[155]Fukuda K, Minamiki T, Minami T, Watanabe M, Fukuda T, Kumaki D and Tokito S 2015 *Adv. Electron. Mater.* 1
[156]Pastorelli F, Schmidt T M, Hösel M, Søndergaard R R, Jørgensen M and Krebs F C 2016 *Adv. Eng. Mater.* 18 51
[157]Holmes N P *et al* 2018 *Chem. Mater.* 30 6521
[158]Sankaran S, Glaser K, Gärtner S, Rödlmeier T, Sudau K, Hernandez-Sosa G and Colsmann A 2016 *Org. Electron.* 28 118
[159]Zhao J, Li Y, Yang G, Jiang K, Lin H, Ade H, Ma W and Yan H 2016 *Nat. Energy* 1
*[160]*Xie C, Tang X, Berlinghof M, Langner S, Chen S, Spath A, Li N, Fink R H, Unruh T and Brabec C J 2018 *ACS Appl. Mater. Interfaces* 10 23225
[161]Landfester K, Montenegro R, Scherf U, Güntner R, Asawapirom U, Patil S, Neher D and Kietzke T 2002 *Adv. Mater.* 14 651

[162]Holmes N P, Burke K B, Sista P, Barr M, Magurudeniya H D, Stefan M C, Kilcoyne A L D, Zhou X, Dastoor P C and Belcher W J 2013 *Solar Energy Mater. Solar Cells* 117 437
*[163]*Holmes N P *et al* 2015 *Solar Energy Mater. Solar Cells* 140 412
[164]Holmes N P *et al* 2016 *Nano Energy* 19 495
[165]Holmes N P, Vaughan B, Williams E L, Kroon R, Anderrson M R, Kilcoyne A L D, Sonar P, Zhou X, Dastoor P C and Belcher W J 2017 *MRS Commun.* 7 67
[166]Pan X *et al* 2018 *Org. Electron.* 59 432
[167]Al-Mudhaffer M F, Griffith M J, Feron K, Nicolaidis N C, Cooling N A, Zhou X, Holdsworth J, Belcher W J and Dastoor P C 2018 *Solar Energy Mater. Solar Cells* 175 77
[168]Gehan T S, Bag M, Renna L A, Shen X, Algaier D D, Lahti P M, Russell T P and Venkataraman D 2014 *Nano Lett.* 14 5238
[169]Bag M, Gehan T S, Renna L A, Algaier D D, Lahti P M and Venkataraman D 2014 *RSC Adv.* 4 45325
[170]Marks M *et al* 2019 *Phys. Chem. Chem. Phys.* Accepted (https://doi.org/10.1039/C8CP07137C)
[171]Griffith M J, Sunahara K, Furube A, Mozer A J, Officer D L, Wagner P, Wallace G G and Mori S 2013 *J. Phys. Chem.* C 117 11885
[172]Ulum S, Holmes N, Darwis D, Burke K, David Kilcoyne A L, Zhou X, Belcher W and Dastoor P 2013 *Solar Energy Mater. Solar Cells* 110 43
[173]Darwis D, Holmes N, Elkington D, David Kilcoyne A L, Bryant G, Zhou X, Dastoor P and Belcher W 2014 *Solar Energy Mater. Solar Cells* 121 99
[174]Xie C *et al* 2018 *Nat. Commun.* 9 5335
[175]Xie C *et al* 2018 *Adv. Energy. Mater* 8
[176]Willmott P 2011 *An Introduction to Synchrotron Radiation: Techniques and Applications* (Chichester: Wiley)
[177]Burke K B, Stapleton A J, Vaughan B, Zhou X, Kilcoyne A L, Belcher W J and Dastoor P C 2011 *Nanotechnology* 22 265710
*[178]*Gu X, Reinspach J, Worfolk B J, Diao Y, Zhou Y, Yan H, Gu K, Mannsfeld S, Toney M F and Bao Z 2016 *ACS Appl. Mater. Interfaces* 8 1687
[179]Rossander L H, Dam H F, Carlé J E, Helgesen M, Rajkovic I, Corazza M, Krebs F C and Andreasen J W 2017 *Energy Environ. Sci.* 10 2411
[180]Dou B *et al* 2018 *ACS Energy Lett.* 3 2558
[181]Carlé J E, Helgesen M, Madsen M V, Bundgaard E and Krebs F C 2014 *J. Mater. Chem.* C 2 1290
[182]Carlé J E *et al* 2017 *Joule* 275
[183]Ammu S, Dua V, Agnihotra S R, Surwade S P, Phulgirkar A, Patel S and Manohar S K 2012 *J. Am. Chem. Soc.* 134 4553
[184]Yin Z P, Huang Y A, Bu N B, Wang X M and Xiong Y L 2010 *Chin. Sci. Bull.* 55 3383
*[185]*Krebs F C, Fyenbo J and Jørgensen M 2010 *J. Mater. Chem.* 20 8994
[186]Oliveira J, Correia V, Sowade E, Etxebarria I, Rodriguez R D, Mitra K Y, Baumann R R and Lanceros-Mendez S 2018 *ACS Appl. Mater. Interfaces* 10 12904
[187]Scheiblin G, Aliane A, Strakosas X, Curto V F, Coppard R, Marchand G, Owens R M, Mailley P and Malliaras G G 2015 *MRS Commun.* 5 507
[188]Hassinen T, Ruotsalainen T, Laakso P, Penttilä R and Sandberg H G O 2014 *Thin Solid Films* 571 212
*[189]*Tong S *et al* 2017 *Flex. Electron*
[190]Forrest S R 2004 *Nat. Commun.* 428 911
*[191]*Mulligan C J, Wilson M, Bryant G, Vaughan B, Zhou X, Belcher W J and Dastoor P C 2014 *Solar Energy Mater. Solar Cells* 120 9
[192]Hoth C N, Schilinsky P, Choulis S A and Brabec C J 2008 *Nano Lett.* 8 2806
[193]Jung S, Sou A, Banger K, Ko D-H, Chow P C Y, McNeill C R and Sirringhaus H 2014 *Adv. Energy. Mater* 4

[194]Youn H, Park H J and Guo L J 2015 *Small* 11 2228
*[195]*Teichler A, Perelaer J and Schubert U S 2013 *J. Mater. Chem.* C 1
[196]Galagan Y, Rubingh J-E J M, Andriessen R, Fan C-C, Blom P W M, Veenstra S C and Kroon J M 2011 *Solar Energy Mater. Solar Cells* 95 1339
*[197]*Kaduwal D, Schleiermacher H-F, Schulz-Gericke J, Kroyer T, Zimmermann B and Würfel U 2014 *Solar Energy Mater. Solar Cells* 124 92
*[198]*Hong S, Lee J, Kang H and Lee K 2013 *Solar Energy Mater. Solar Cells* 112 27
[199]Välimäki M, Jansson E, Korhonen P, Peltoniemi A and Rousu S 2017 *Nanoscale Res. Lett.* 12 117
[200]Apilo P *et al* 2018 *RRL Solar* 2 1700160
[201]Blankenburg L, Schultheis K, Schache H, Sensfuss S and Schrödner M 2009 *Solar Energy Mater. Solar Cells* 93 476
[202]Machui F, Lucera L, Spyropoulos G D, Cordero J, Ali A S, Kubis P, Ameri T, Voigt M M and Brabec C J 2014 *Solar Energy Mater. Solar Cells* 128 441
[203]Lucera L, Machui F, Kubis P, Schmidt H D, Adams J, Strohm S, Ahmad T, Forberich K, Egelhaaf H-J and Brabec C J 2016 *Energy Environ. Sci.* 9 89
[204]Krebs F C, Fyenbo J, Tanenbaum D M, Gevorgyan S A, Andriessen R, Remoortere B V, Galagan Y and Jørgensen M 2011 *Energy Environ. Sci.* 4 4116
[205]Krebs F C, Espinosa N, Hösel M, Søndergaard R R and Jørgensen M 2014 *Adv. Mater.* 26 29
[206]Larsen-Olsen T T, Andersen T R, Dam H F, Jørgensen M and Krebs F C 2015 *Solar Energy Mater. Solar Cells* 137 154
[207]Griffith M J, Cooling N A, Vaughan B, O'Donnell K M, Al-Mudhaffer M F, Al-Ahmad A, Noori M, Almyahi F, Belcher W J and Dastoor P C 2015 *Energy Technol.* 3 428
[208]Andersen T R *et al* 2016 *J. Mater. Chem.* A 4 15986
[209]CHEP Press Release 2017 *A Powerful Innovation: University of Newcastle and CHEP Sign a Partnership to Test Printed Solar Cell Panels in a Commercial Environment* (Vantage)
[210]Lee E-K *et al* 2017 *Adv. Electron. Mater.* 3
[211]Katsuhara M *et al* 2010 *J. Soc. Inf. Display* 18
[212]Vladimirov I, Chow C, Strudwick A-J, Kowalsky W, Schwab M G, Kälblein D and Weitz R T 2015 *Phys. Status Solidi* a 212 2059
*[213]*Søndergaard R R, Hösel M and Krebs F C 2013 *J. Polym. Sci.* B 51 16
[214]Sirringhaus H, Kawase T, Friend R H, Shimoda T, Inbasekaran M, Wu W and Woo E P 2000 *Science* 290 2123
*[215]*Sirringhaus H, Kawase T and Friend R H 2011 *MRS Bull.* 26 539
[216]Sele C W, von Werne T, Friend R H and Sirringhaus H 2005 *Adv. Mater.* 17 997
[217]Cho J H, Lee J, Xia Y, Kim B, He Y, Renn M J, Lodge T P and Frisbie C D 2008 *Nat. Mater.* 7 900
[218]Rogers J A, Someya T and Huang Y 2010 *Science* 327 1603
[219]Sekitani T, Takamiya M, Noguchi Y, Nakano S, Kato Y, Sakurai T and Someya T 2007 *Nat. Mater.* 6 413
[220]Someya T, Sekitani T, Iba S, Kato Y, Kawaguchi H and Sakurai T 2004 *Proc. Natl Acad. Sci.* 101 9966
[221]Sekitani T, Noguchi Y, Zschieschang U, Klauk H and Someya T 2008 *Proc. Natl Acad. Sci.* 105 4976
[222]Sekitani T, Noguchi Y, Hata K, Fukushima T, Aida T and Someya T 2008 *Science* 321 1468
[223]Matsuhisa N, Inoue D, Zalar P, Jin H, Matsuba Y, Itoh A, Yokota T, Hashizume D and Someya T 2017 *Nat. Mater.* 16 834
[224]Thompson B and Yoon H-S 2013 *IEEE Sens. J.* 13 4256
[225]Griffith M J, Cooling N A, Elkington D C, Muller E, Belcher W J and Dastoor P C 2014 *Appl. Phys. Lett.* 105 143301
[226]Lochner C M, Khan Y, Pierre A and Arias A C 2014 *Nat. Commun.* 5 5745

[227] Griffith M J, Willis M, Kumar P, Holdsworth J L, Bezuidenhout H, Zhou X, Belcher W J and Dastoor P C 2016 *ACS Appl. Mater. Interfaces* 8 7926

[228] Fukuda K, Takeda Y, Yoshimura Y, Shiwaku R, Tran L T, Sekine T, Mizukami M, Kumaki D and Tokito S 2014 *Nat. Commun.* 5 4147

[229] Fraboni B, Ciavatti A, Basiricò L and Fraleoni-Morgera A 2014 *Faraday Discuss.* 174 219

[230] Fraboni B, Fraleoni-Morgera A and Zaitseva N 2016 *Adv. Mater.* 26 2276

[231] Lai S, Cosseddu P, Basiricò L, Ciavatti A, Fraboni B and Bonfiglio A 2017 *Adv. Electron. Mater* 3 1600409

[232] Cosseddu P, Lai S, Barbaro M and Bonfiglio A 2012 *Appl. Phys. Lett.* 100 1063

[233] Ciavatti A, Basiricò L, Fratelli I, Lai S, Cosseddu P, Bonfiglio A, Anthony J E and Fraboni B 2018 *Adv. Funct. Mater.* 1806119

[234] Intaniwet A, Mills C A, Shkunov M, Thiem H, Keddie J L and Sellin P J 2009 *J. Appl. Phys.* 106 064513

[235] Boroumand F A, Zhu M, Dalton A B, Keddie J L and Sellin P J 2007 *Appl. Phys. Lett.* 91 033509

[236] Newman C R, Sirringhaus H, Blakesley J C and Speller R D 2007 *Appl. Phys. Lett.* 91 142105

[237] Agostinelli T, Campoy-Quiles M, Blakesley J C, Speller R, Bradley D D C and Nelson J 2008 *Appl. Phys. Lett.* 93 20

[238] Büchele P *et al* 2015 *Nat. Photon.* 9

[239] Thirimanne H M *et al* 2018 *Nat. Commun.* 9 2926

[240] Bihar E, Deng Y, Miyake T, Saadaoui M, Malliaras G G and Rolandi M 2016 *Sci. Rep.* 6 27582

[241] Berto M *et al* 2018 *Adv. Biosyst.* 2

[242] Magliulo M, De Tullio D, Vikholm-Lundin I, Albers W M, Munter T, Manoli K, Palazzo G and Torsi L 2016 *Anal. Bioanal. Chem.* 408 3943

[243] Ghezzi D, Antognazza M R, Dal Maschio M, Lanzarini E, Benfenati F and Lanzani G 2011 *Nat. Commun.* 2 166